Exothermic Dark Matter with a Dark Higgs: The LZ 248 keV Event and the Galactic Center Excess

Pyungwon Ko (KIAS QUC)

ICFP 2026, Beijing, China, Oct 24-26 (2026)

Based on arXiv:2610.25423 [hep-ph]
with Jinheung Kim[1] Jongkuk Kim[2]
[1]School of Physics, KIAS [2]Kangwon National University

Outline

0. BSM model building along the SM construction (Personal Viewpoint)

1. Introduction: the LZ 248 keV event and what it asks of dark matter

2. Model: a dark $U(1)_X$ gauge theory with a dark Higgs

3. Method: from the Lagrangian to the LZ rate

4. Results: LZ fit, excited-state decays, Galactic Center excess

5. Discussion: why the dark Higgs cannot be dropped

Lesson from π decay

- You can easily consider $\pi \to l\nu$ ($l = \mu, e$). I bet you will start with $\mathscr{L} \sim \pi \bar{l} \nu$ (dim-4). But we know it is wrong!
- Correct EFT will be $\mathscr{L} \sim \frac{1}{\Lambda} \partial_\mu \pi \; \bar{l} \gamma^\mu \nu$ (dim-5) , but it is not the end of the story
- Correct Answer: $\mathscr{L} = \frac{G_F}{\sqrt{2}} V_{ud} \; (\bar{u} d)_{V-A} (\bar{\mu} \nu)_{V-A}$ (dim-6) →SM by Weinberg, Salam
- A simple EFT may not be enough!
- Keep in mind that something similar can happen for DM models or in any BSM studies!

Then, how to construct $\mathscr{L}$ for data anomalies?

My talk at NEXUS 2026, TDLI last month

- Identify local symmetries, as well as particle contents that can accommodate data anomalies [No global symmetries are imposed in the beginning, as in the SM]
- Write down all possible (super) renormalizable operators with the presumed gauge symmetries → Renormalizable Lagrangian with Unitarity
- Impose Anomaly Cancellation and Realistic Yukawa's
- Identify the accidental global symmetries [NB: Global Sym's in the SM are all accidental]
- Check if Higher Dim Op's conserve/break the accidental global sym's
- Minimal Setup without Theo/Math Inconsistency!!! EFT or Simplified Models are Not Enough & Could Be Misleading!

“Anomaly free” as an example: Before GIM

- Weinberg Model for u, d, s (+ Cabbibo) : $(u_L, d_L \cos\theta_c + s_L \sin\theta_c)^T$, $u_R, d_R, s_R,$
- Predicts FCNC ~ FCCC : $\Gamma(K^+ \to \mu^+\nu_\mu) \sim \Gamma(K^0 \to \mu^+\mu^-)$, in contradiction to the exp data. What is going on?
- Where is the other orthogonal combination, $(-d_L \sin\theta_c + s_L \cos\theta_c)$?

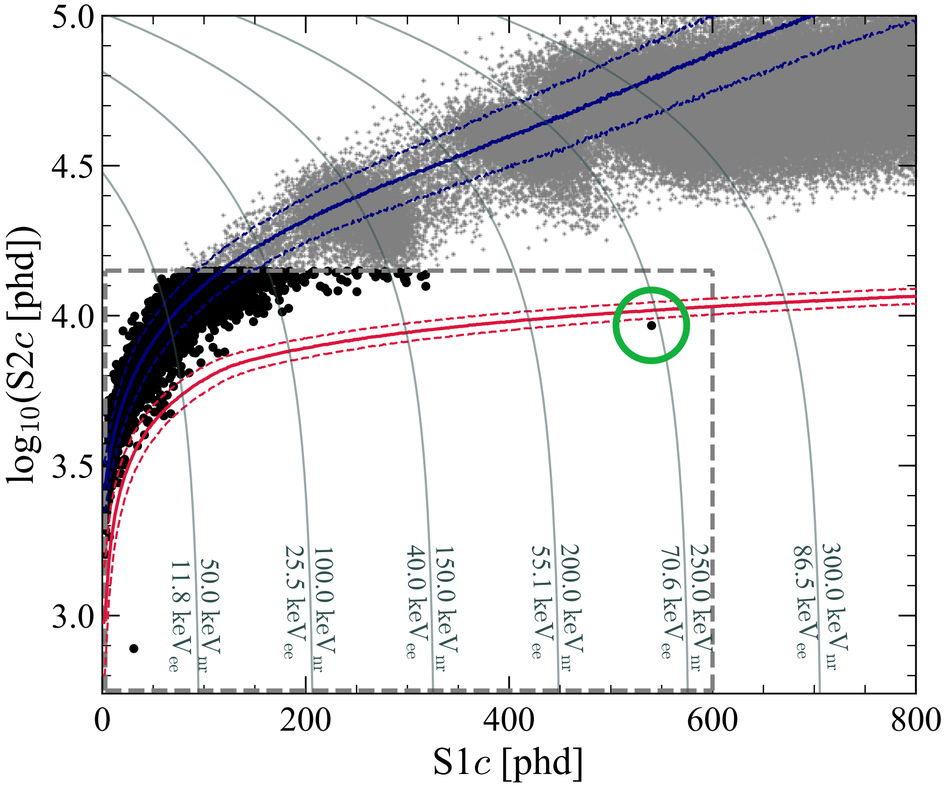
“Anomaly free” as an example: GIM (1970)

- GIM proposed to introduce the 4th quark, “charm”, as the SU(2) partner of the 2nd combination
- FCNC=0 @ tree level, and induced at loops
- $m_c \sim 1.5$ GeV explains Δm_K (Gaillard, Lee, Rossner, 1974), and confirmed by discovery of J/ψ in 1974 !
- In retrospect, large FCNC is a wrong prediction of anomalous gauge theory for 3 quark flavors, which is not a healthy theory

The LZ 248 keV event

LZ extended its nuclear-recoil search to high recoil energies: an exposure of 2.84 tonne-years, searched up to ≈ 270 keV. One event lies in the NR band, at E_R = 248 ± 23_stat ± 23_sys keV, with a global significance of 2.6σ. The ROI holds 1710 events in all, and the high-energy sideband holds none.

I will take it as a signal for DM-N scattering



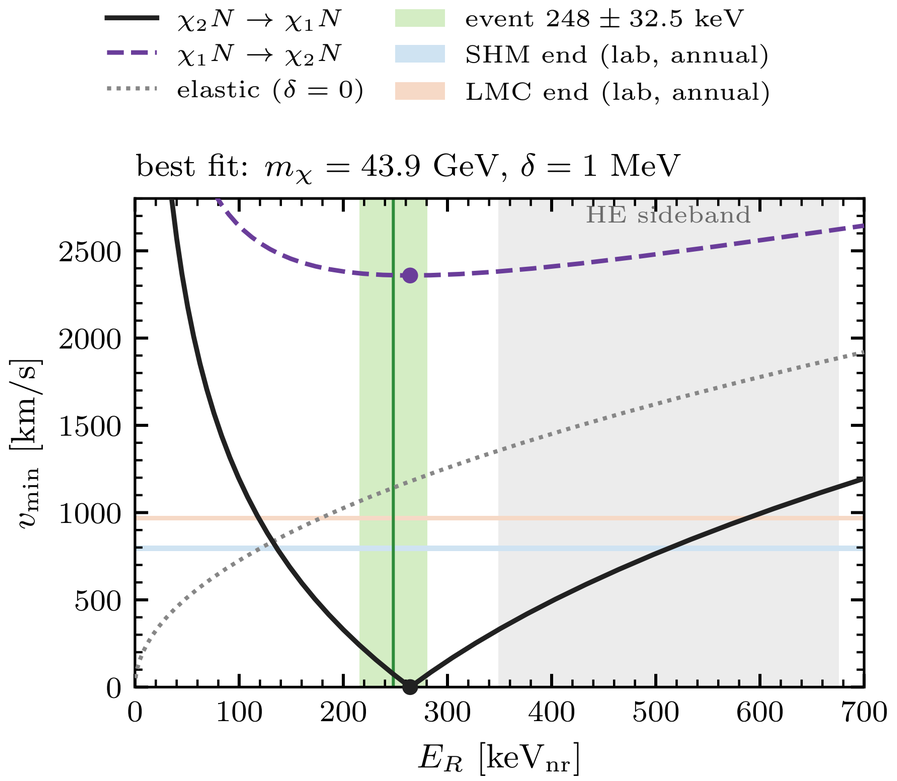
LZ Collaboration, arXiv:2609.02823, Fig. 4 (circle added)

Exothermic inelastic DM

Elastic scattering gives a spectrum that falls steeply with E_R. Endothermic up-scattering $\chi_1 N \to \chi_2 N$ reaches higher energies, but only with fast DM. Exothermic down-scattering $\chi_2 N \to \chi_1 N$ releases δ, so even slow DM recoils hard:

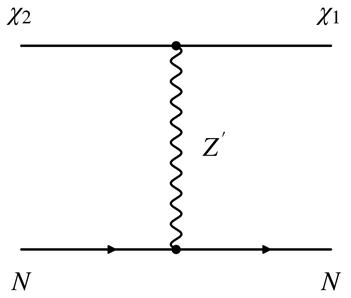
$$v_{\min}(E_R) = \frac{1}{\sqrt{2 m_N E_R}} \left| \frac{m_N E_R}{\mu_N} - \delta \right|$$

The minimum velocity vanishes at $E_R^* = \mu_N \delta / m_N$ (≈ 264 keV at the best fit), and the recoils fill a window around it.

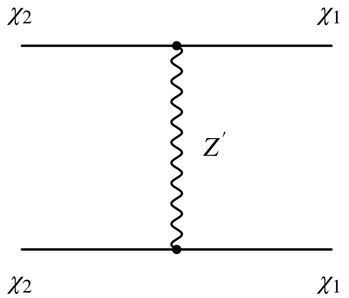


What exothermic DM needs

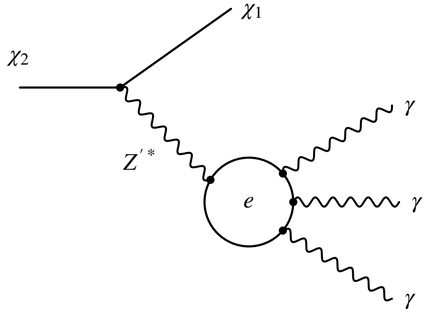
Exothermic scattering needs a splitting δ between two nearly degenerate states and a population of the heavier state χ_2 that survives until today. In a gauge theory, δ cannot be a bare mass: a Majorana mass for a charged Dirac fermion breaks the dark U(1), so δ must come from the vacuum expectation value of a field with charge two. And the Z' that lets χ_2 scatter also converts and destroys it, so f_2 must be computed.



scattering $\chi_2 N \to \chi_1 N$



conversion $\chi_2\chi_2 \to \chi_1\chi_1$ (+ crossed)



decay $\chi_2 \to \chi_1 + 3\gamma$

Earlier exothermic fits (δ as a parameter or from a scalar outside the relic and γ-ray calculations; f_2 set near 1/2 or evolved with conversion alone): de Lima 2026; Baer & Barger 2026; Gemmell, Hooper & Krnjaic 2026; Deka 2026.

Dark $U(1)_X$ with a dark Higgs

$$\begin{aligned}\mathcal{L} = \mathcal{L}_{\rm SM} &- \frac{1}{4}X_{\mu\nu}X^{\mu\nu} - \frac{\sin\epsilon}{2}X_{\mu\nu}B^{\mu\nu} + \bar{\chi}(i\not{D} - m_D)\chi \\ &- \frac{1}{\sqrt{2}}\left(y\,\Phi^\dagger\overline{\chi^c}\chi + \text{H.c.}\right) + (D_\mu\Phi)^\dagger(D^\mu\Phi) + m_\Phi^2\Phi^\dagger\Phi \\ &- \lambda_\Phi(\Phi^\dagger\Phi)^2 - \lambda_{H\Phi}(H^\dagger H)(\Phi^\dagger\Phi)\end{aligned}$$

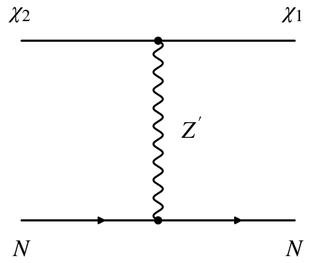
The dark sector has the gauge boson X_μ , a Dirac fermion χ with $Q_\chi = 1$ and a dark Higgs Φ with $Q_\Phi = 2$, coupled to the SM through the kinetic mixing ϵ and the Higgs portal $\lambda_{H\Phi}$. Because $Q_\Phi = 2Q_\chi$, the Yukawa term is gauge invariant: with $\Phi = (v_\Phi + \phi_0)/\sqrt{2}$, one vacuum value gives $m_X = 2g_X v_\Phi$ and $\delta = 2yv_\Phi$, splitting χ into two nondegenerate Majorana states $\chi_{1,2}$ ($m_\chi \equiv m_{\chi_1}$). And the original dark $U(1)_X$ is spontaneously broken into its subgroup Z_2. The remnant Z_2 keeps χ_1 stable even in the presence of blackholes.

Local Z_2 dark matter model: Baek, Kim & Ko 2020. See also Baek, Ko, Park (2014) for Local Z_2 scalar DM for GCE.

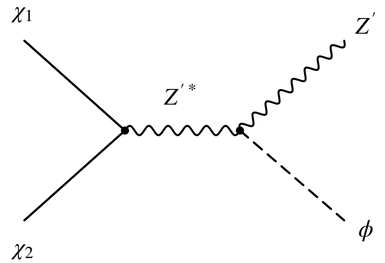
Local Z_2 means $U(1) \to Z_2$, describes inelastic DM in a dark-gauge invariant way. Similarly for local Z_3 scalar DM, P.Ko, Y.Tang (2014)

Fields and processes

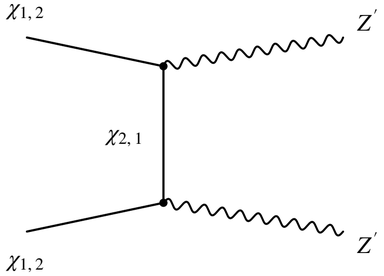
$$\mathcal{L} \supset -i\frac{g_X}{2}\left(Z'_\mu + \epsilon s_W Z_\mu\right)\left(\bar{\chi}_2\gamma^\mu\chi_1 - \bar{\chi}_1\gamma^\mu\chi_2\right)$$
$$-\frac{g_X\delta}{2m_{Z'}}\,\phi\left(\bar{\chi}_2\chi_2 - \bar{\chi}_1\chi_1\right)$$



Exothermic scattering $\chi_2 N \to \chi_1 N$



coannihilation $\chi_1\chi_2 \to Z'\phi$ (dark Higgsstrahlung)

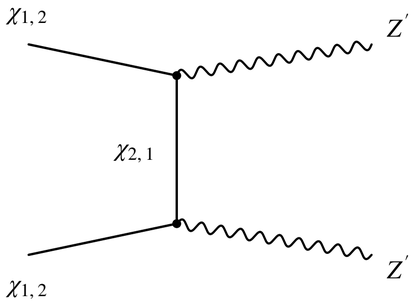


annihilation $\chi_i\chi_i \to Z'Z'$ (only t-channel shown; u and s-channel ϕ on the next slide)

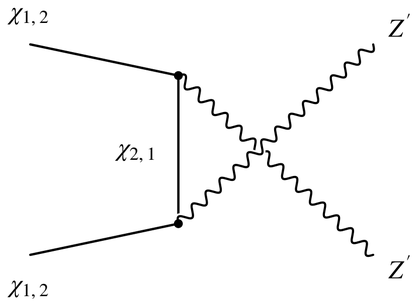
The Z' links χ_1 and χ_2 only, so the leading Z' exchange on nuclei is inelastic; the ϕ-mediated elastic part is negligible. The same couplings give the decays $\chi_2 \to \chi_1 + \nu\bar{\nu}$ and $\chi_1 + 3\gamma$ and the conversion $\chi_2\chi_2 \to \chi_1\chi_1$.

Where the dark Higgs enters

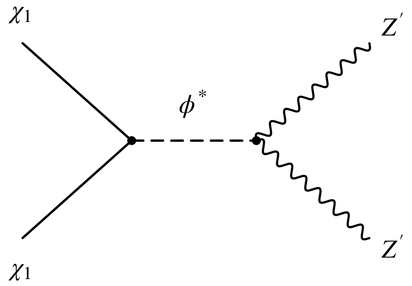
Its vacuum value gives $m_{Z'} = 2g_X v_\Phi$, the splitting $\delta = 2yv_\Phi$ and the Z_2 that keeps χ_1 stable. Its radial mode ϕ cancels the energy growth of the Z'_L amplitudes, opens $\chi_1\chi_2 \to Z'\phi$ next to $\chi_i\chi_i \to Z'Z'$ in the relic density, and on the high branch, shapes the GCE photons through $\phi \to b\bar{b}$.



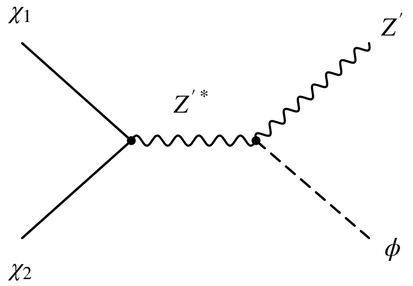
t: χ exchange



u: χ exchange



s: ϕ exchange
cancels the growth

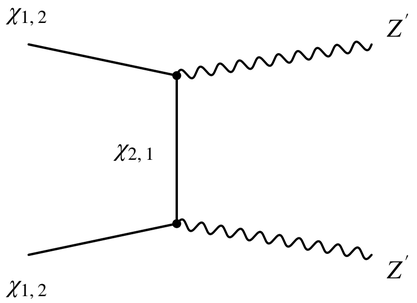


$\chi_1\chi_2 \to Z'\phi$: relic, GCE

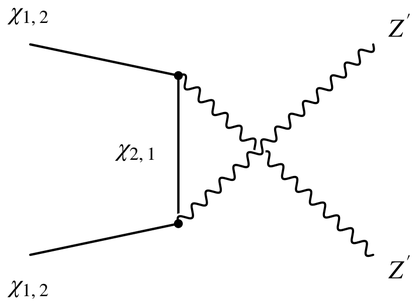
These are the threads of the talk: gauge invariance and unitarity (theory), the relic density (cosmology) and the Galactic Center (astrophysics). At the end we ask whether ϕ can be dropped.

Where the dark Higgs enters

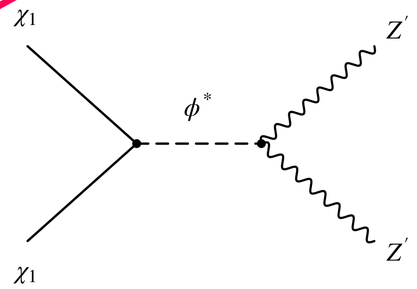
Its vacuum value gives $m_{Z'} = 2g_X v_\Phi$, the splitting $\delta = 2yv_\Phi$ and the Z_2 that keeps χ_1 stable. Its radial mode ϕ cancels the energy growth of the Z_L' amplitudes, opens $\chi_1\chi_2 \to Z'\phi$ next to $\chi_i\chi_i \to Z'Z'$ in the relic density, and on the high branch, shapes the GCE photons through $\phi \to b\bar{b}$.



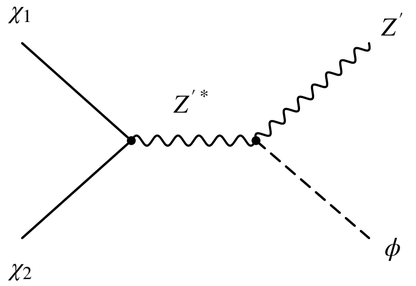
t: χ exchange



u: χ exchange



s: ϕ exchange
cancels the growth



$\chi_1\chi_2 \to Z'\phi$: relic, GCE

These are the threads of the talk: gauge invariance
(cosmology) and the Galactic Center (astrophysics
dropped.

These two diagrams involve dark Higgs,
And not possible in Stueckelberg!

Relic density

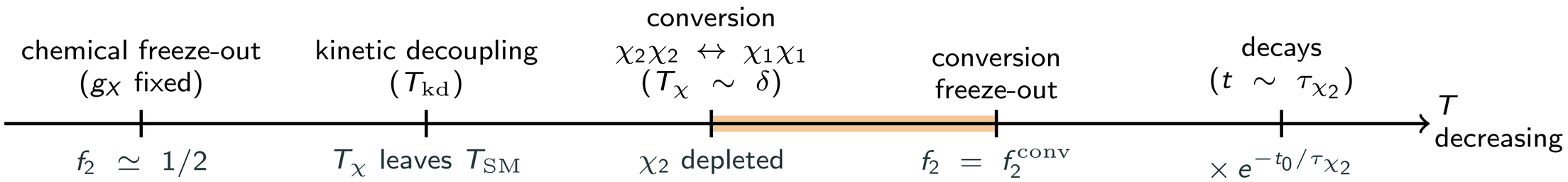
We scan $(m_\chi, \delta, m_{Z'})$ with $m_\phi = m_{Z'}$, ϵ = 10^{-4} and s_α = 10^{-6}, and fix g_X at every point by Ωh^2 = 0.120 (micrOMEGAs). Two channels set it, $\chi_i\chi_i \to Z'Z'$ and the dark Higgsstrahlung $\chi_1\chi_2 \to Z'\phi$, and for $m_\phi = m_{Z'}$ below m_χ both are open. Closing $Z'\phi$ with $m_\phi = 10m_\chi$ needs a larger g_X:

$$g_X = 0.111 \longrightarrow 0.149 \quad (\times\ 1.34)$$

high-branch LZ best fit, with and without the $Z'\phi$ channel

Ωh^2: Planck 2018.

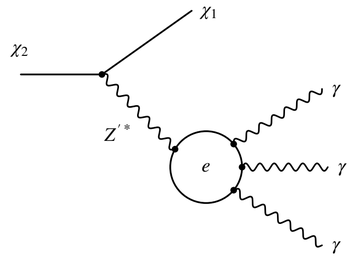
The excited fraction f_2



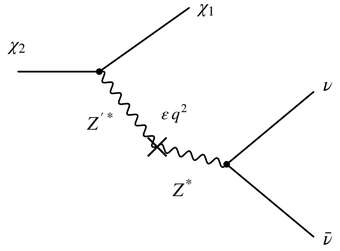
The excited fraction $f_2 \equiv n_{\chi_2}/(n_{\chi_1} + n_{\chi_2})$ follows from a Boltzmann equation with conversion, bath scattering and decays (equations in the backup). The conversion runs at the dark matter temperature T_χ , below kinetic decoupling, and we compute it nonperturbatively. The decays act last and give today's value, $f_2 = f_2^{\rm conv} e^{-t_0/\tau_{\chi_2}}$ (next slide).

χ_2 decays

The remnant Z_2 lets χ_2 decay only into χ_1, through an off-shell Z' into SM particles. For $\delta < 2m_e$, the fast channel $\chi_2 \to \chi_1 e^+ e^-$ is closed, and two slow ones remain: $\chi_1 + 3\gamma$ through an electron loop and $\chi_1 \nu\bar{\nu}$ through the Z admixture of the Z' . Both widths scale as $\epsilon^2 g_X^2 / m_{Z'}^4$, like $\sigma_{\chi p}$, and grow steeply with δ (δ⁹ for $\nu\bar{\nu}$, δ¹³ for 3γ at $\delta \ll 2m_e$). They are negligible during the conversion, so they only multiply its frozen value by $e^{-t_0/\tau_{\chi 2}}$.



χ₂ → χ₁+3γ



χ₂ → χ₁νν̄ (schematic mixing insertion)

	$m_{Z'}$ [GeV]	$\tau_{\chi 2}$ [s]	$f_2^{\rm conv}$	f_2 today
low	0.986	4.24×10^{16}	0.0252	8.89×10^{-7}
high	26.33	2.37×10^{22}	0.497	$\simeq f_2^{\rm conv}$

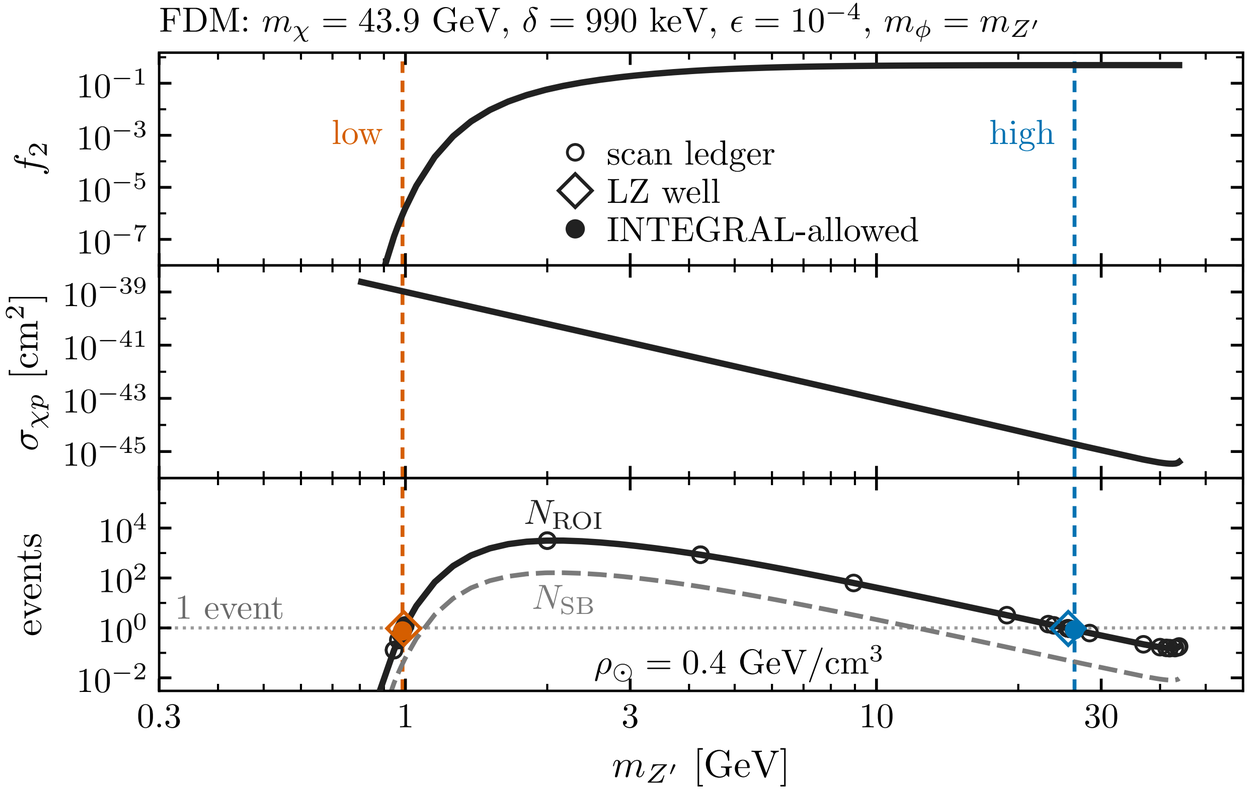
INTEGRAL-allowed benchmarks, (43.9 GeV, 990 keV)

On the low branch χ₂ decays before today, $e^{-t_0/\tau_{\chi 2}} = 3.52 \times 10^{-5}$; on the high branch $\tau_{\chi_2} \gg t_0$ and the decays leave f_2 unchanged.

Widths (backup): Batell, Pospelov & Ritz 2009; Krnjaic et al. 2025; one loop near 2m_e: McDermott, Patel & Ramani 2018.

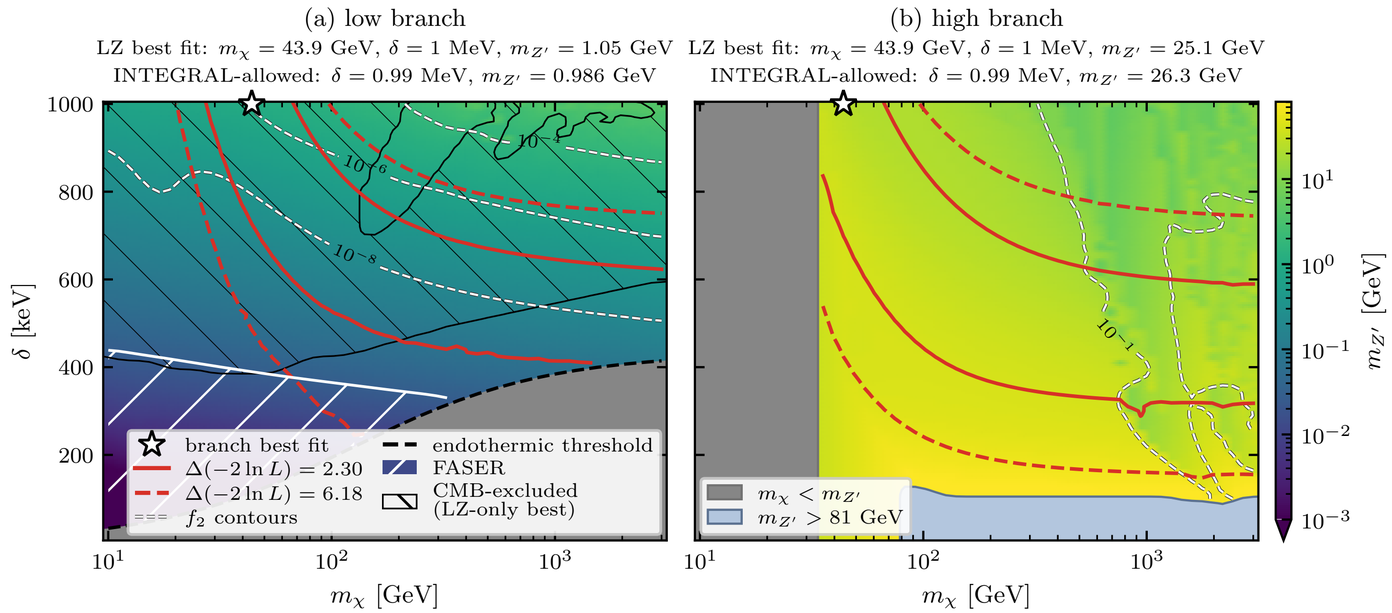
Two branches in m_Z′

For $q^2 \lesssim m_{Z'}^2$, (m_χ, δ) approximately fixes the shape of the spectrum, and $m_{Z'}$ mainly sets its normalization. For a small $m_{Z'}$, fast conversion and decays suppress f_2 ; for a large $m_{Z'}$, $f_2 \simeq 1/2$ but $\sigma_{\chi p} \propto g_X^2/m_{Z'}^4$ falls. So $N_{\rm ROI}$ rises and then falls, and it reaches one event twice: the low and the high branch.



Benchmark cell (43.9 GeV, 990 keV), m_ϕ = m_Z′, ρ⊙ = 0.4 GeV/cm³; scan ledger: scan points, LZ well: LZ-only minimum

LZ fit: two branches



Color: best-fit m_Z′; white dashed: f_2; red: Δ(–2 ln $\mathscr{L}$) = 2.30, 6.18 (nominal coverage); black hatching: CMB-excluded; white hatching: FASER; black dashed: endothermic threshold

Both branches have their minimum at (43.9 GeV, 1000 keV) with $N_{\mathrm{ROI}} \simeq 0.94$, but the low branch sits at $m_{Z'}$ = 1.050 GeV with $f_2 \simeq 1.54 \times 10^{-6}$ and the high branch at $m_{Z'}$ = 25.08 GeV with f_2 = 0.4971. The favored region is a valley of nearly constant E_R^* that runs up to TeV masses; its low-mass end is set by $\delta < 2m_e$. The fit treats the event as signal, and the minimum lies at the upper end of the δ scan.

Excited-state decays: INTEGRAL and CMB

The 3γ width shares the factor $\epsilon^2 g_X^2 / m_{Z'}^4$ with the LZ rate, so for given (m_χ, δ) the LZ rate fixes today's MeV photon flux from $\chi_2 \to \chi_1 + 3\gamma$; the INTEGRAL/SPI limit moves the benchmarks to $\delta = 990$ keV.

On the low branch, the large pre-decay population $f_2^{\rm conv}$ decays in the dark ages: the CMB excludes the benchmark and most of the region near the minimum. On the high branch $\tau_{\chi_2} \gg t_0$.

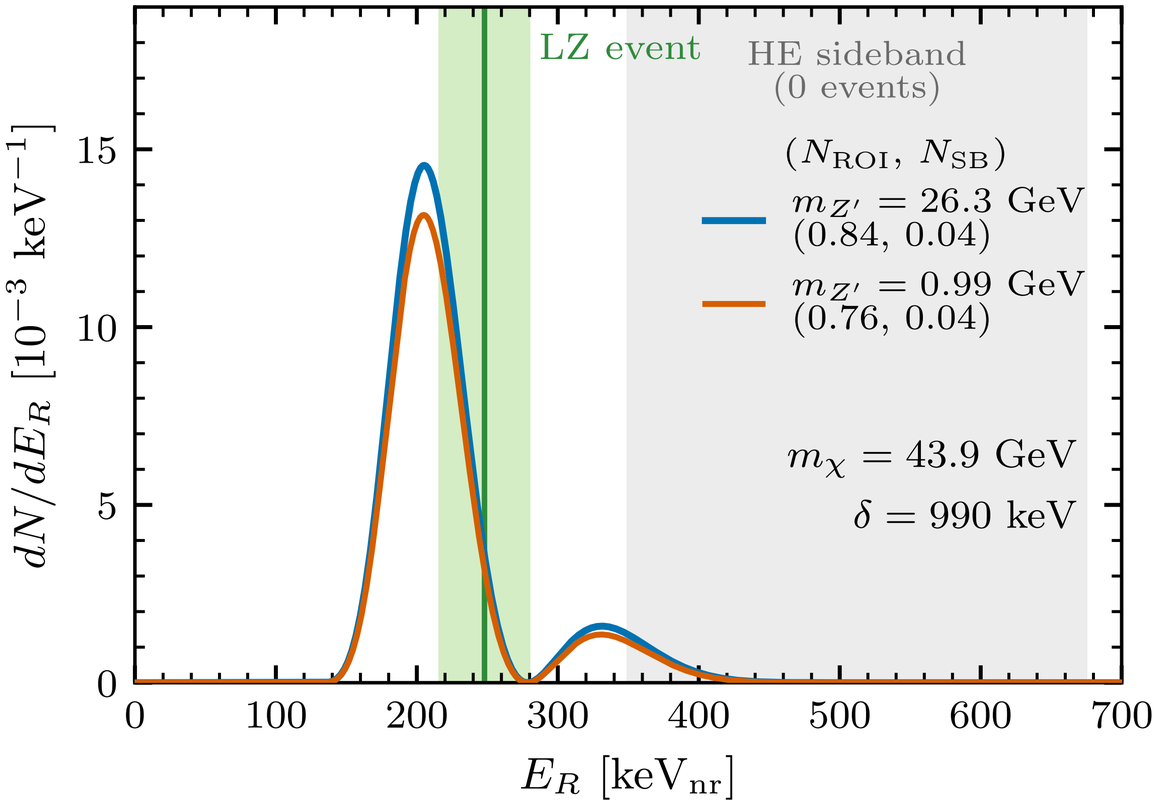
$$\frac{\Gamma(\chi_2 \to \chi_1 + 3\gamma)}{\sigma_{\chi p}} \quad \text{depends only on} \quad (m_\chi, \delta)$$

The CMB excludes the low branch near its minimum

INTEGRAL/SPI: Krnjaic et al. 2025, rescaled to our f_2 and halo. CMB: Slatyer & Wu 2017.

Recoil spectra at the benchmarks

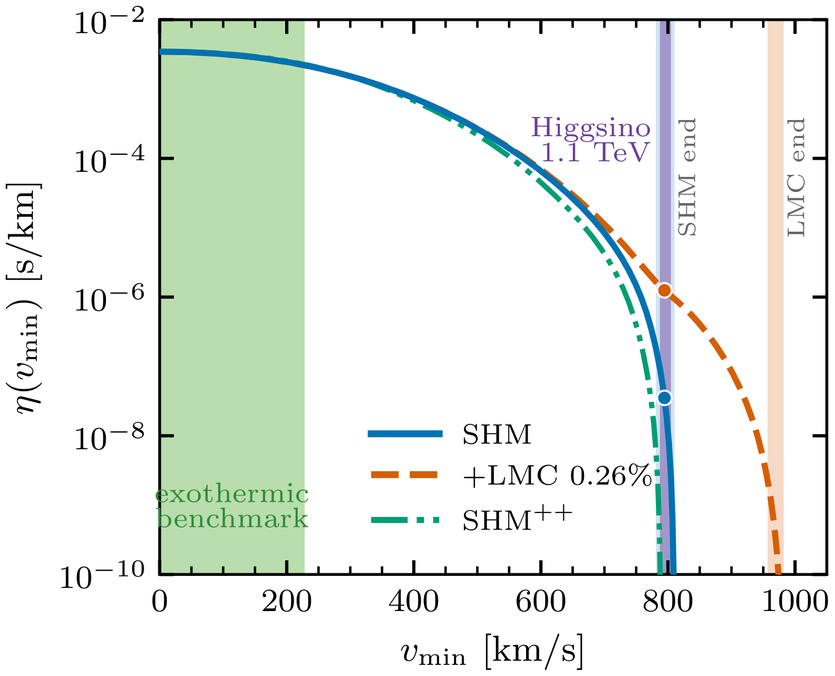
The benchmarks sit at (43.9 GeV, 990 keV), where INTEGRAL allows them. They give $N_{\rm ROI} = 0.757$ on the low branch and 0.838 on the high branch, with N_SB ≲ 0.0439 in the empty sideband. Near the event $v_{\rm min} \lesssim 228$ km/s, far below the Earth-frame maximum of ≈ 800 km/s, so the signal comes from the bulk of the halo.

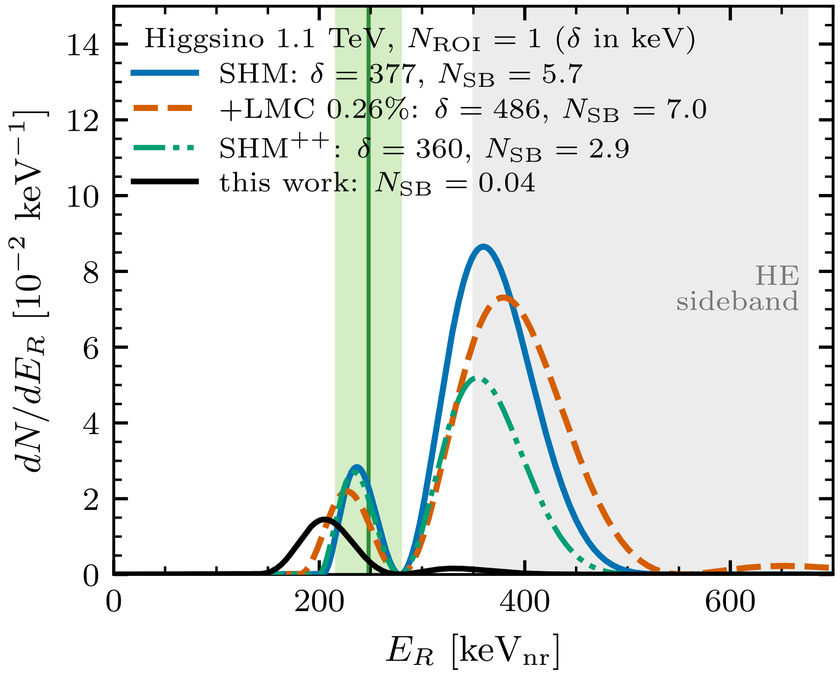


true E_R, before efficiency and smearing; the dip is the second zero of the xenon form factor

Comparison: the endothermic Higgsino

For the endothermic 1.1 TeV Higgsino, $v_{\min} \geq \sqrt{(2\delta/\mu_N)}$ puts the event at the end of the halo, where halo models disagree (left, δ tuned for the SHM); retuned to one ROI event for each halo, it puts 3–7 events into the empty sideband (right).



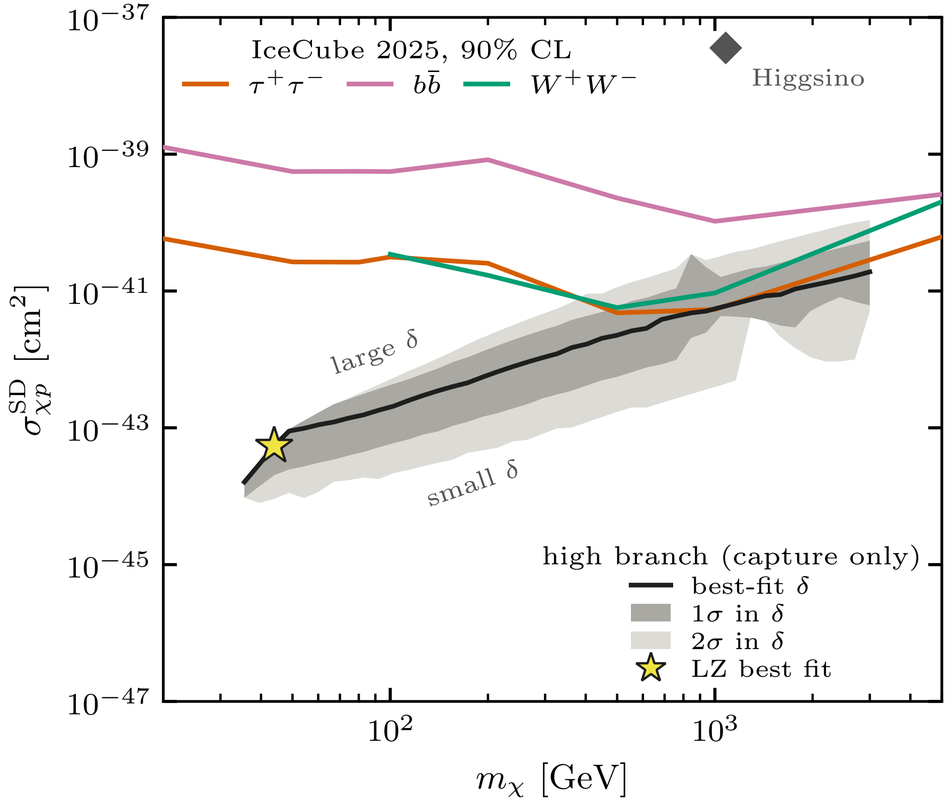


Higgsino: Rodd et al. 2026; Fan & Reece 2026; Langhoff 2026. SHM^{++}: Evans et al. 2019. LMC: Smith-Orlik et al. 2023.

Solar neutrinos, colliders, BBN

Solar neutrino searches exclude neither benchmark. On the high branch, capture at the benchmark gives σ^eff⊙ = 4.45×10^{-44} cm², two orders of magnitude below the IceCube limit of $\approx 3 \times 10^{-41}$ cm²; on the low branch, the muons and mesons from Z′ decays stop in the Sun before they decay.

Since $Z' \to \chi_1\chi_2$ is closed, the Z' decays visibly, and its coupling lies below the BaBar and KLOE limits near the low branch and the LHCb and CMS limits near the high branch. At the benchmarks the dark Higgs decays before BBN for $\sin\alpha = 10^{-6}$.

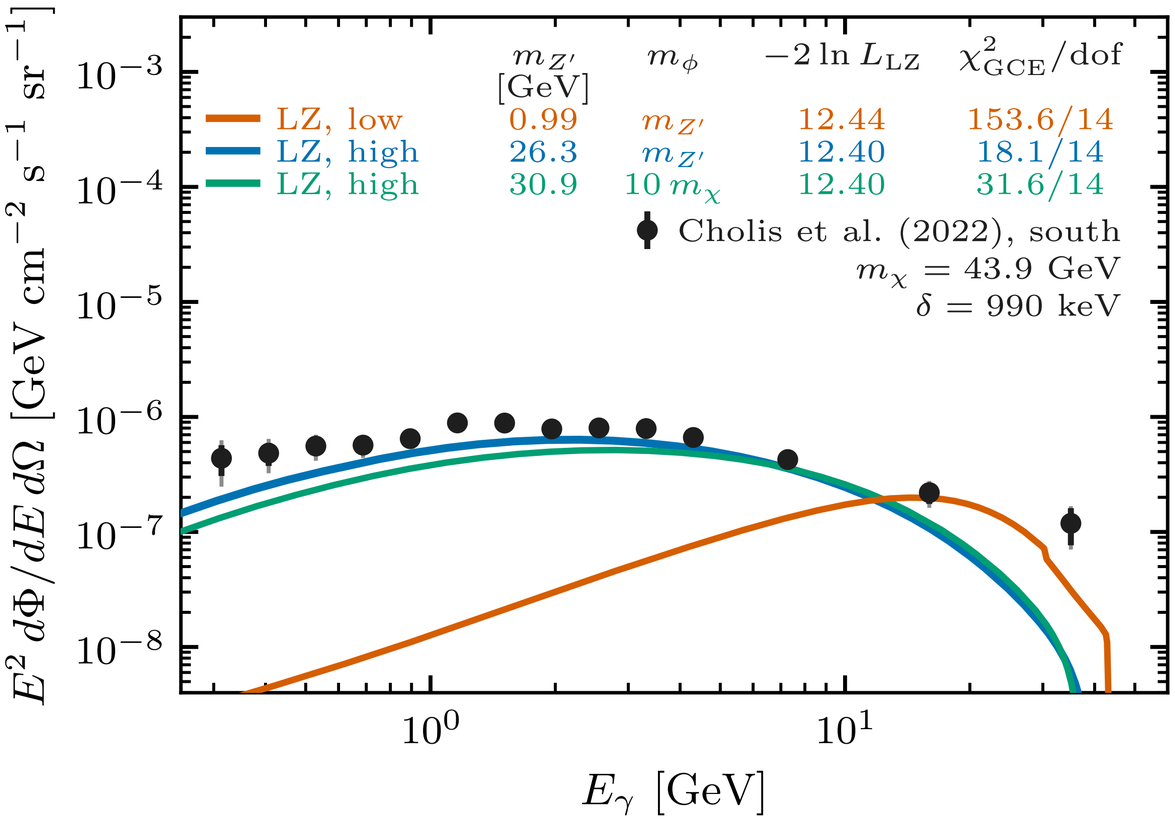


High branch along the LZ valley, capture only, IceCube convention (ρ⊙ = 0.3 scan); star: LZ-only best fit of that scan (text: benchmark, ρ⊙ = 0.4), diamond: Higgsino

IceCube 2025 (τ⁺τ⁻); BaBar 2014; KLOE-2 2018; LHCb 2020; CMS 2020; ϕ decays: Winkler 2019.

The Galactic Center excess

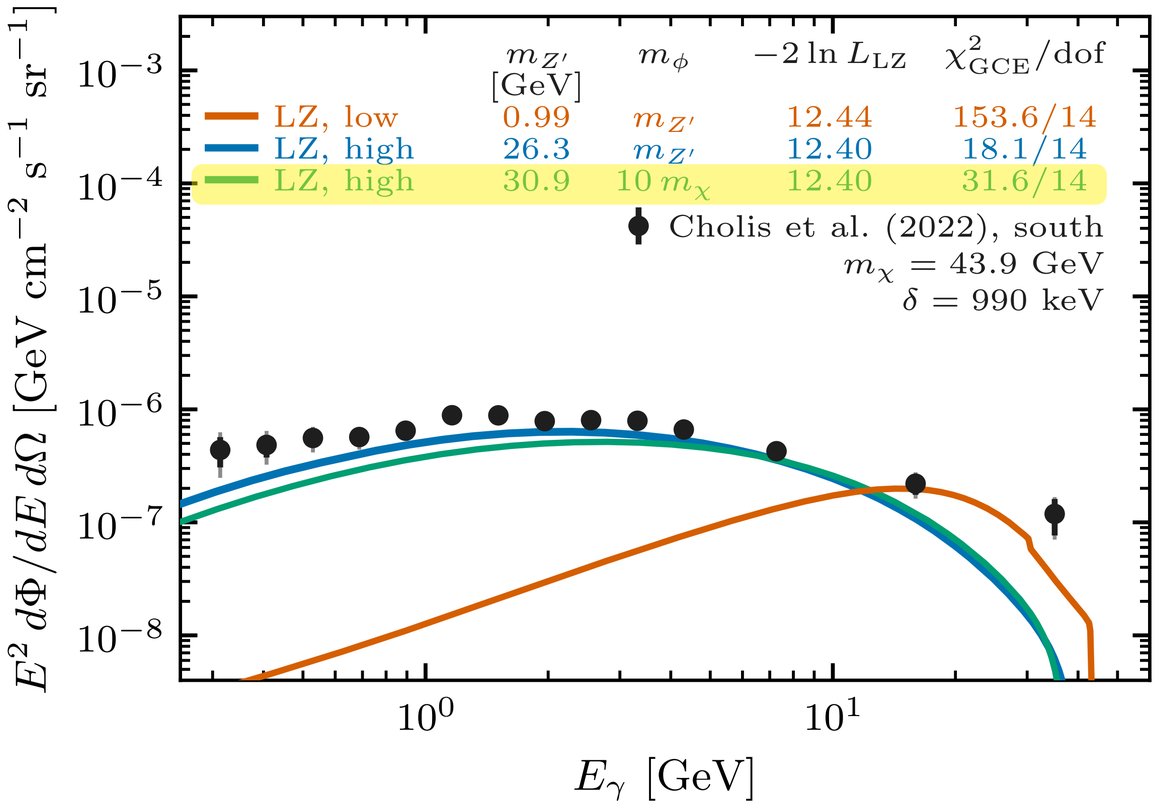
On the high branch, the benchmark, with nothing fitted to the gamma rays, gives χ^2/dof = 18.1/14, as good as the best generic $b\bar{b}$ fit at 17.1/12. With a free normalization, A = 1.07±0.10, consistent with the relic σv. The low branch gives 153.6/14, worse than no signal at 130.7.



Southern-sky GCE spectrum, its covariance and the generic $b\bar{b}$ fit: Cholis et al. 2022; one halo for LZ, INTEGRAL and the GCE. Joint LZ + GCE proposal: Gemmell, Hooper & Krnjaic 2026.

GCE without the dark Higgs

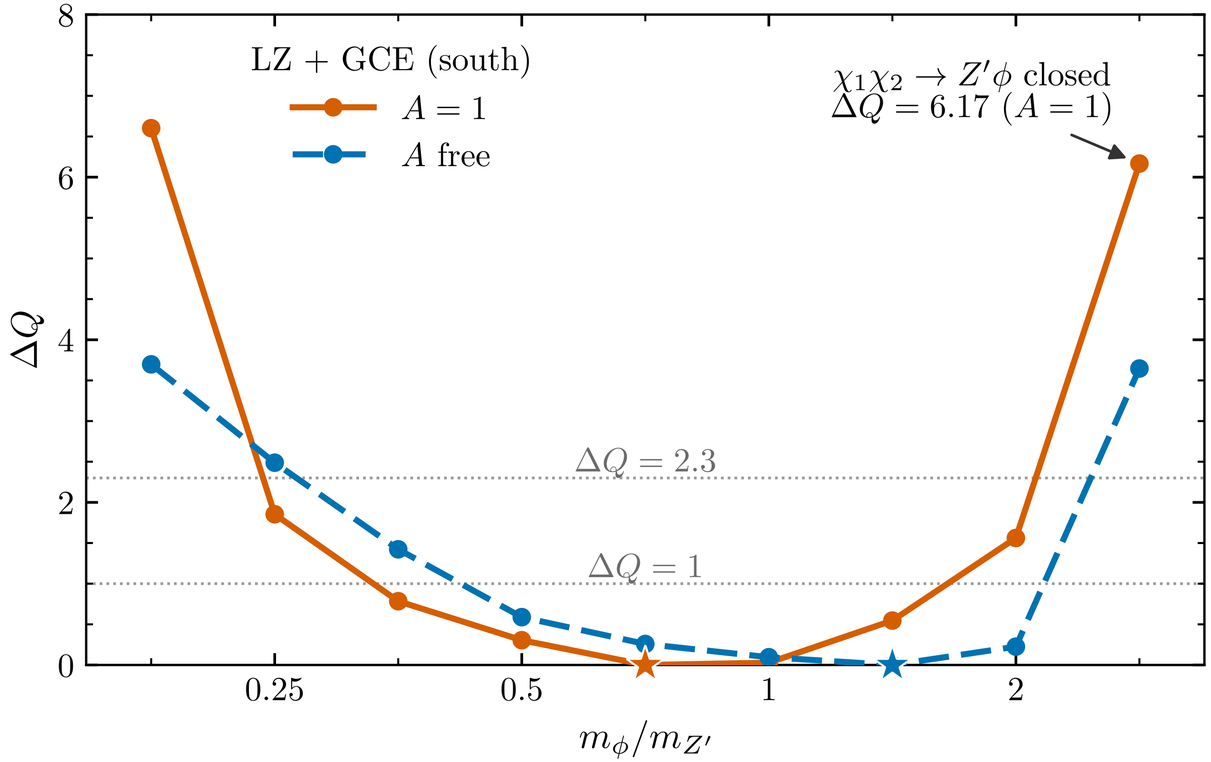
Closing $\chi_1\chi_2 \to Z'\phi$ with the heavy-ϕ proxy $m_\phi = 10 m_\chi$ raises the relic coupling from g_X = 0.1109 to 0.1526, and the fit (green) worsens from χ^2/dof = 18.1/14 to 31.6/14. With $f_2 \simeq 1/2$, the $Z'\phi$ channel is active, and its photons come mostly from $\phi \to b\bar{b}$; with $Z'Z'$ alone, the fit is worse.



Freeing m_Z′ and m_ϕ

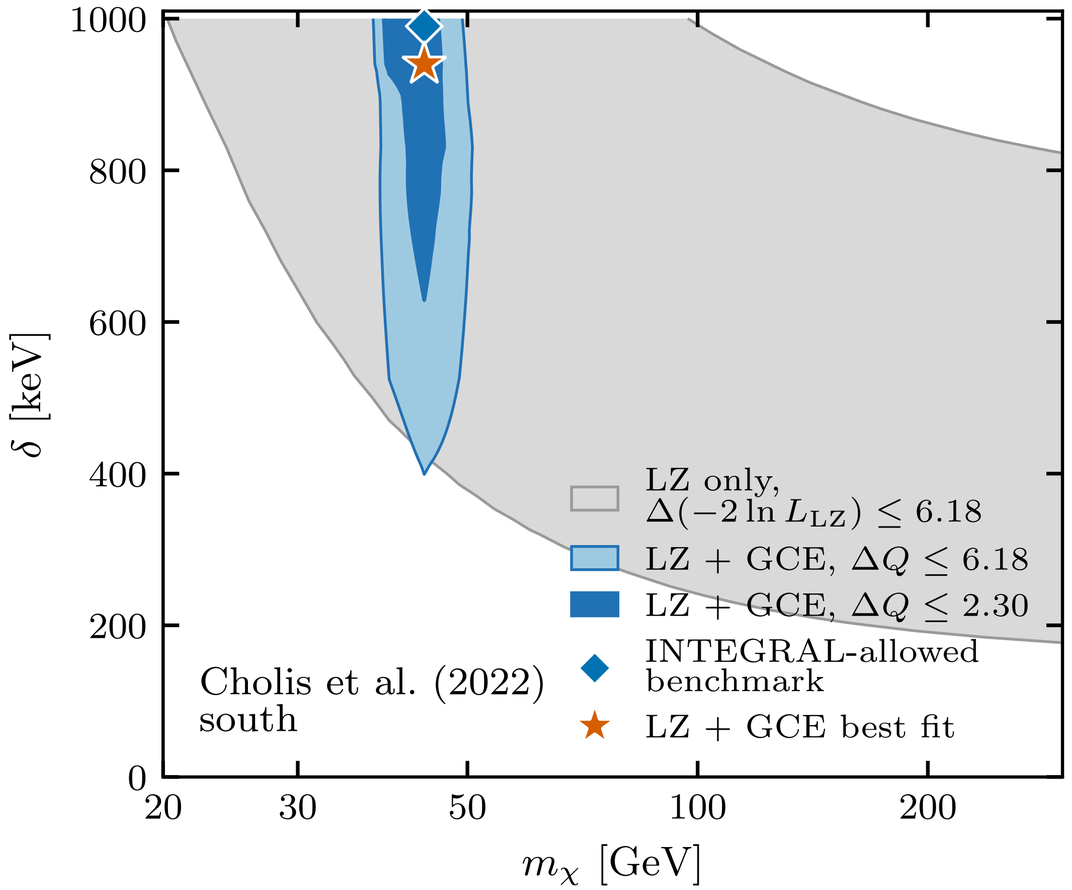
$$Q = -2 \ln \mathcal{L}_{\rm LZ} + \chi^2_{\rm GCE}$$

We minimize Q over $(m_\chi, \delta, m_{Z'}, m_\phi)$ on the southern sky, with A fixed and no INTEGRAL limit. The best fit lies beside the benchmark at $m_\phi/m_{Z'} = 0.71$, at almost no cost to LZ, and $\Delta Q \leq 1$ holds for 0.35 ≤ $m_\phi/m_{Z'}$ ≤ 1.4 (0.5–2 with a free A, dashed). At $m_\phi/m_{Z'} = 2.8$, where $Z'\phi$ is closed, ΔQ = 6.17.



LZ and GCE: one spot

The gray region is LZ alone, a long valley of nearly constant E_R^* . The blue region adds the southern-sky GCE spectrum, which pins m_χ to the low-mass part of the valley. The joint best fit of this scan over $m_\phi/m_{Z'} \in \{1/2, 1, 2\}$, without the INTEGRAL limit (star), lies beside the INTEGRAL-allowed benchmark (diamond).



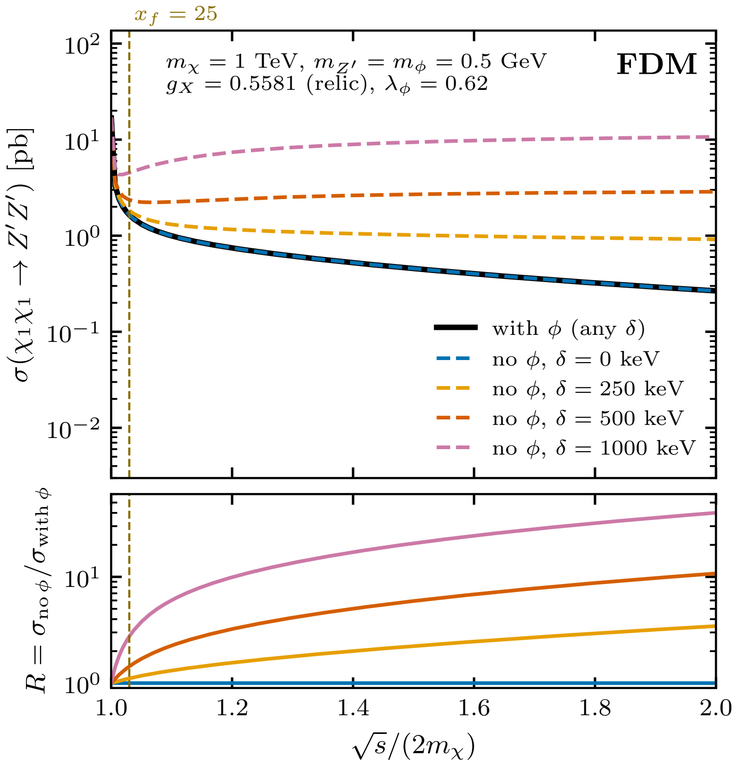
Dark Higgs: theory

Usual Pseudo-Dirac DM

$$\mathcal{L}(\text{no } \Phi) \supset \frac{1}{2} m_{Z'}^2 Z'_\mu Z'^\mu - \frac{1}{4}\delta(\overline{\chi^c}\chi + \text{H.c.})$$

$$|\mathcal{M}(\chi_1\chi_1 \to Z'_L Z'_L)| \sim \frac{2g_X^2\,\delta}{m_{Z'}^2}\sqrt{s}$$

Can ϕ be dropped? In the simplified model, the Z' mass is a Stückelberg term, and the δ term breaks $U(1)_X$, restored only by a Stückelberg dressing ($m_\phi \to \infty$). Its Z'_L amplitudes grow with $\sqrt{s}$, so it is an EFT valid below $\sqrt{s_{\text{cut}}} = 4\pi m_{Z'}^2/(g_X^2\delta)$; in our model the s-channel ϕ cancels the growth. At our benchmarks, the growth is small at freeze-out $m_{Z'}^2/\delta \gg 2m_\chi$; it matters for a light Z' and a heavy χ, as in the figure.



Upper: $\sigma(\chi_1\chi_1 \to Z'Z')$ with and without ϕ ; lower: R = σ_(no ϕ)/σ_(with ϕ); vs √s/2m_χ at m_χ = 1 TeV, m_Z′ = m_ϕ = 0.5 GeV, g_X = 0.56

Fits with δ as a parameter: de Lima 2026; Baer & Barger 2026; Deka 2026. Energy growth: Ko, Matsui & Tang 2020; Jeong, Ko & Zheng 2026. Figure: Fig. S1 (left) of our paper.

Dark Higgs: perturbativity and data

In the Higgs completion $\lambda_\Phi \simeq 2g_X^2 m_\phi^2/m_{Z'}^2$, so $\lambda_\Phi \lesssim 2\pi$ bounds $m_\phi \lesssim \sqrt{\pi} m_{Z'}/g_X$. On the low branch this lies far below the $Z'\phi$ threshold $m_\phi < 2m_\chi - m_{Z'}$: ϕ cannot close the channel. On the high branch, ϕ can close it but cannot decouple; the $m_\phi = 10m_\chi$ proxy already needs $\lambda_\Phi \approx 9.42$.

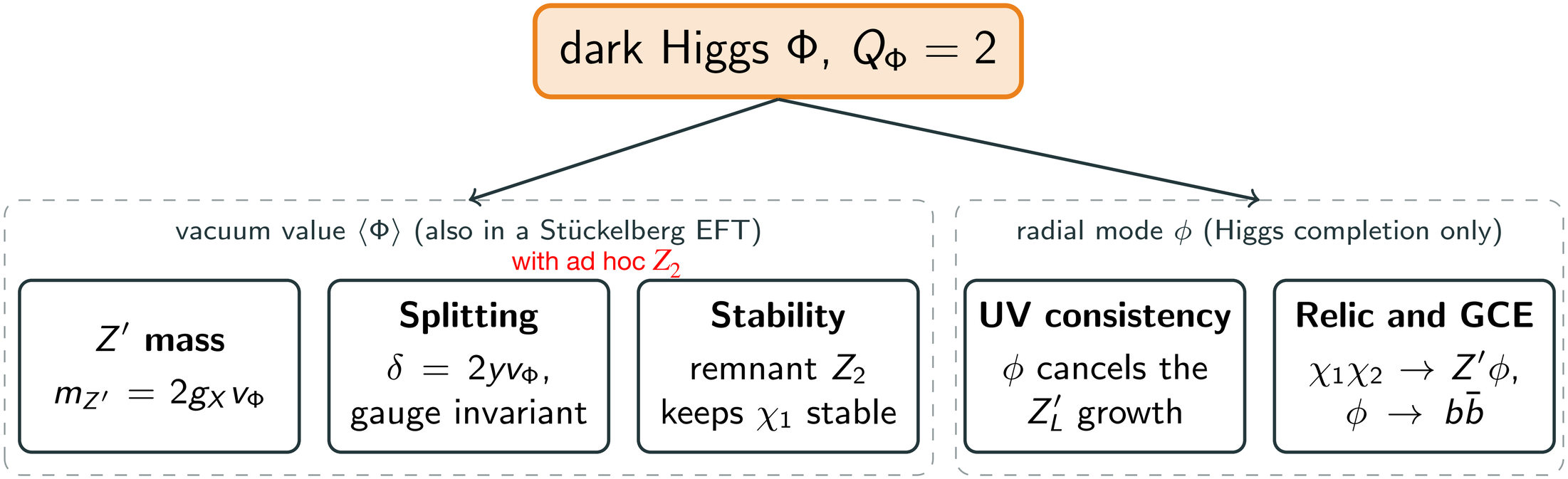
	low	high
$m_{Z'}$ [GeV]	0.986	26.33
g_X	0.1162	0.1109
$\sqrt{\pi}\, m_{Z'}/g_X$ [GeV]	15	421

INTEGRAL-allowed benchmarks, m_χ = 43.9 GeV

On the high branch the data decide. LZ alone is indifferent (–2 ln $\mathcal{L}$ = 12.396 and 12.396 with and without $Z'\phi$), but closing $Z'\phi$ raises the relic g_X from 0.1109 to 0.1526 and worsens the GCE fit from 18.1/14 to 31.6/14; in the four-mass fit with A = 1, ΔQ = 6.17 once the channel closes.

Perturbative unitarity: Kahlhoefer et al. 2016.

One field, five jobs



The dark Higgs is not a decoration of the dark photon model:
it keeps the model consistent in the UV and makes it fit the GCE !!

Summary

If the LZ event is dark matter, exothermic scattering explains it with a splitting and a surviving excited state. Gauge invariance makes the splitting the vacuum value of a charge-2 field; in the renormalizable completion this is a dark Higgs, which also gives $m_{Z'}$ and the stabilizing Z_2, and whose radial mode cannot decouple while staying perturbative. With f_2 computed, the CMB excludes the low branch near its minimum. LZ alone does not fix m_ϕ , but on the high branch a dark Higgs near $m_{Z'}$ fits the southern-sky GCE (adopted covariance) at the relic normalization.

In a renormalizable and gauge invariant theory, the dark Higgs boson is not optional, and the southern-sky GCE prefers it near $m_{Z'}$!

How to test it

A future MeV γ-ray telescope can see the 3γ flux that the LZ rate fixes. Argon detectors would see the signal below the first form-factor zero, and the existing XENONnT and PandaX-4T data can probe it in an extended energy window. Dwarf spheroidals and AMS-02 antiprotons test the GCE interpretation.

Thank you

Argon: de Lima 2026; Baer & Barger 2026 (arXiv:2609.06153); Baer & Barger 2026, argon (arXiv:2609.15782). Xenon: Dent & Newstead 2026.



Jongkuk Kim (Kangwon NU)



Jinheung Kim (KIAS)

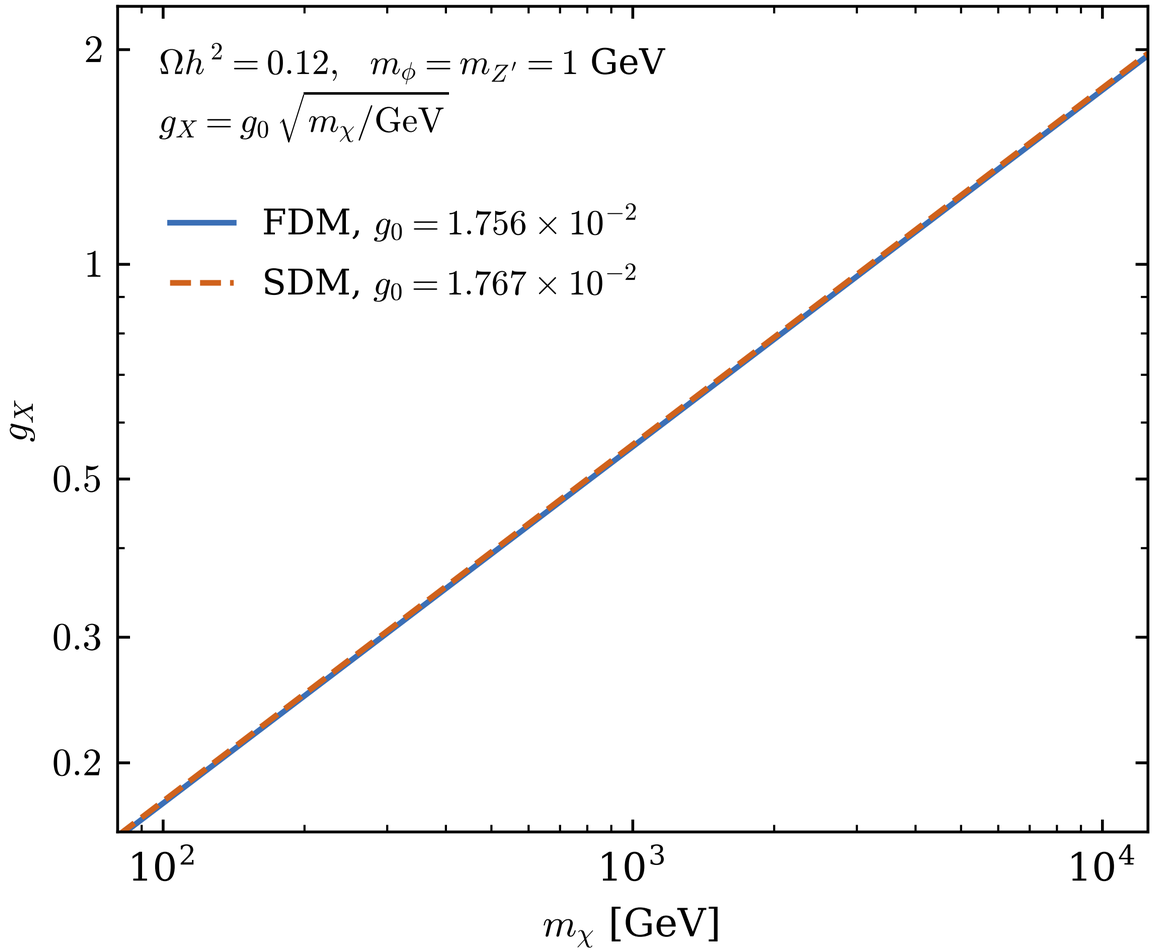
Backup: benchmark table

(m_χ, δ) = (43.9 GeV, 990 keV), $\epsilon = 10^{-4}$, $\sin\alpha = 10^{-6}$, $\rho_\odot$ = 0.4 GeV/cm^3; γ flux at the INTEGRAL limit

	low	high	high, $m_\phi = 10\, m_\chi$
$m_{Z'}$ [GeV]	0.986	26.33	30.88
m_ϕ [GeV]	$= m_{Z'}$	$= m_{Z'}$	439.1
g_X	0.1162	0.1109	0.1526
λ_Φ	0.0270	0.0246	9.42
$T_{\rm kd}$ [GeV]	0.0229	0.654	0.650
$f_2^{\rm conv}$	0.0252	0.497	0.496
f_2	8.89×10^{-7}	0.4974	0.4961
τ_{χ_2} [s]	4.24×10^{16}	2.37×10^{22}	2.37×10^{22}
$N_{\rm ROI}$	0.757	0.838	0.837
$N_{\rm SB}$	0.0367	0.0439	0.0439
$-2\ln\mathcal{L}$	12.436	12.396	12.396
$\Delta(-2\ln\mathcal{L})$ from the LZ-only best	0.10	0.06	0.06
$\langle\sigma v\rangle_{\rm eff}$ [cm^3/s]	2.20×10^{-26}	2.30×10^{-26}	2.25×10^{-26}
$\chi^2_{\rm GCE}/{\rm dof}$, south	153.6/14	18.1/14	31.6/14
CMB ratio	48.8	0.0015	0.0015

Backup: relic coupling

The coupling that gives $\Omega h^2 = 0.120$ grows as $g_X \propto \sqrt{m_\chi}$ at fixed $m_{Z'}$ and m_ϕ, as expected for $\langle \sigma v \rangle \propto g_X^4 / m_\chi^2$. The fermion (FDM) and scalar (SDM) versions of the model need almost the same coupling at these masses.



relic coupling at $m_\phi = m_{Z'} = 1\mathrm{GeV}$ (micrOMEGAs)

Backup: thermal history

$$\frac{df_2}{dt} = -\, n_\chi \,\langle \sigma_{22\to 11} v \rangle \left[f_2^2 - \xi^2(T_\chi)\,(1-f_2)^2 \right] - \Gamma_\downarrow(T_{\rm SM})\, f_2 + \Gamma_\uparrow(T_{\rm SM})\,(1-f_2) - \Gamma_{\chi_2} f_2$$

$$\frac{dT_\chi}{dt} + 2HT_\chi = 2\gamma(T_{\rm SM})\,(T_{\rm SM} - T_\chi)$$

Here ξ(T) ≡ (1+δ/m_χ)^(3/2)e^(–δ/T) is the equilibrium ratio n_χ₂/n_χ₁, and Γ↑ = ξ(T_SM) Γ↓ by detailed balance. Conversion removes χ₂ at the rate ⟨σ_(22→11)v⟩ n_χ₂² per volume, and γ and Γ↓ come from χ_(1,2) ℓ → χ_(2,1) ℓ on charged leptons, with the same Z′ amplitudes. Below T_kd, T_χ ∝ T_SM²/T_kd, reheated by the conversions. We solve without Γ_χ₂ and then set $f_2 = f_2^{\rm conv} e^{(-t_0/\tau_{\chi_2})}$.

Backup: kinetic decoupling

Lepton scattering keeps $T_\chi = T_{\rm SM}$ early, through $dT_\chi/dt + 2HT_\chi = 2\gamma(T_{\rm SM})(T_{\rm SM} - T_\chi)$.

At late times, without the conversions, this defines $T_{\rm kd}$:

$$T_\chi(T_{\rm SM}) = \frac{T_{\rm SM}^2}{T_{\rm kd}} \left(\frac{g_{*s}(T_{\rm SM})}{g_{*s}(T_{\rm kd})} \right)^{2/3} \qquad (T_{\rm SM} < T_{\rm kd})$$

Below $T_{\rm kd}$, conversions heat the dark sector (common $\chi_{(1,2)}$ temperature):

$$T_\chi = T_\chi{}^{(0)} \left(\frac{1 - f_2^{\rm eq}}{1 - f_2^{\rm kd}} \right)^{2/3} \exp\left[-\frac{2}{3} \left(\frac{f_2^{\rm eq}\,\delta}{T_\chi} - \frac{f_2^{\rm kd}\,\delta}{T_{\rm kd}} \right) \right]$$

This is used only to locate the conversion freeze-out. The benchmarks have $T_{\rm kd}$ = 0.0229 GeV (low) and 0.654 GeV (high). The bath holds charged leptons only, and the high-branch $T_{\rm kd}$ lies in the QCD crossover, where $f_2 \simeq 1/2$ is insensitive to $T_{\rm kd}$.

Backup: nonperturbative conversion

$$V(r) = \begin{pmatrix} 0 & -\alpha_X e^{-m_{Z'} r}/r \\ -\alpha_X e^{-m_{Z'} r}/r & 2\delta \end{pmatrix}$$

$$\sigma_{22\to 11}(v) = (\pi/k_2^2) \sum_\ell w_\ell \, (2\ell+1) \, |S_{12}^{(\ell)}|^2$$

For $\alpha_X m_\chi / m_{Z'} \gtrsim 1$, multiple Z' exchanges matter: they suppress the rate below Born and make it oscillate in $m_{Z'}$. We solve the coupled channels $(\chi_1\chi_1, \chi_2\chi_2)$ with $\alpha_X = g_X^2/4\pi$ and ϕ neglected, with the incoming wave in $\chi_2\chi_2$ only and w_l = 1/2 (3/2) for even (odd) ℓ. The correction is small at our benchmarks.

Ko, Matsui & Tang 2020; Baer & Barger 2026.

Backup: LZ likelihood

$$\ln \mathcal{L} = \ln \mathrm{Pois}\left(1 \mid N_{\mathrm{ROI}}(\vec{\theta})\right) + \ln \mathrm{Pois}\left(0 \mid N_{\mathrm{SB}}(\vec{\theta})\right) + \ln p(248\ \mathrm{keV} \mid \vec{\theta}),$$

$$\frac{dN}{dE_R} = \mathcal{E}\,\frac{\rho_\odot}{m_\chi}\,\frac{Z^2\sigma_{\chi p}}{2\mu_{\chi p}^2}\,F^2(q^2)\left(\frac{m_{Z'}^2}{q^2+m_{Z'}^2}\right)^2\left[f_1\,\eta(v_{\mathrm{min}}^{\mathrm{endo}}) + f_2\,\eta(v_{\mathrm{min}}^{\mathrm{exo}})\right],$$

$$\sigma_{\chi p} = 4\alpha_{\mathrm{EM}}\epsilon^2 c_W^2 g_X^2 \mu_{\chi p}^2 / m_{Z'}^4$$

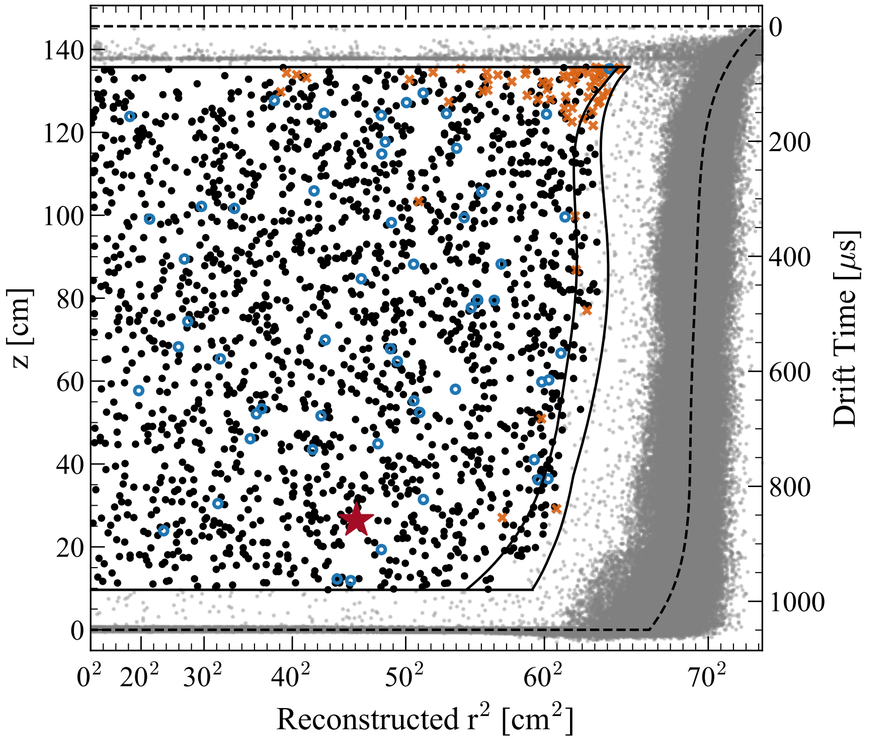
The likelihood combines one event in the ROI, none in the sideband, and the spectrum at the event, where p is the ROI spectrum smeared by the event's 32.5 keV resolution. The parameters are $\{m_\chi, \delta, m_{Z'}\}$, with g_X from the relic density and f_2 computed. The rate uses the SHM velocity distribution with $\rho_\odot$ = 0.4 GeV/cm³ of the gNFW halo that also serves INTEGRAL and the GCE, and the regions are drawn at $\Delta(-2\ln\mathcal{L})$ = 2.30 and 6.18.

Halo: Cholis et al. 2022. Contour coverage for a single event is not calibrated.

Backup: LZ likelihood inputs

$$-2\ln\mathcal{L}_B = 2(N_{\mathrm{ROI}} + B_{\mathrm{ROI}}) - 2\ln[N_{\mathrm{ROI}}\, p_s + B_{\mathrm{ROI}}\, p_b] + 2(N_{\mathrm{SB}} + B_{\mathrm{SB}})$$

N_ROI uses the LZ NR efficiency over the WS ROI S1c = 3–600 phd, and N_{SB} the window 800 < S1c < 1700 phd with an acceptance from the LZ energy scale. The spectral term p is the efficiency-weighted ROI spectrum ⊗ a Gaussian of width 32.5 keV. The background density p_b at the event is not published, so we test it from $p_b = 0$ to signal-like, and the best fit stays at (43.9 GeV, 1000 keV) in every case.



LZ Collaboration, arXiv:2609.02823, Fig. 3 (star: event of interest)

Backup: backgrounds, LMC and $\rho_\odot$

With the expected LZ backgrounds, tested from no background at the event to a signal-like shape, the best fit stays at (43.9 GeV, 1000 keV). An LMC component changes –2 ln $\mathscr{L}$ by ≈ 0.016. One halo serves LZ, INTEGRAL and the GCE, and since the GCE flux scales as $\rho_\odot^2$, its normalization A depends on the chosen $\rho_\odot$.

$\rho_\odot$ [GeV/cm^3]	A, south
0.4	1.06 ± 0.10
0.3	1.85 ± 0.18

LZ-only high-branch best fit, refitted for each $\rho_\odot$

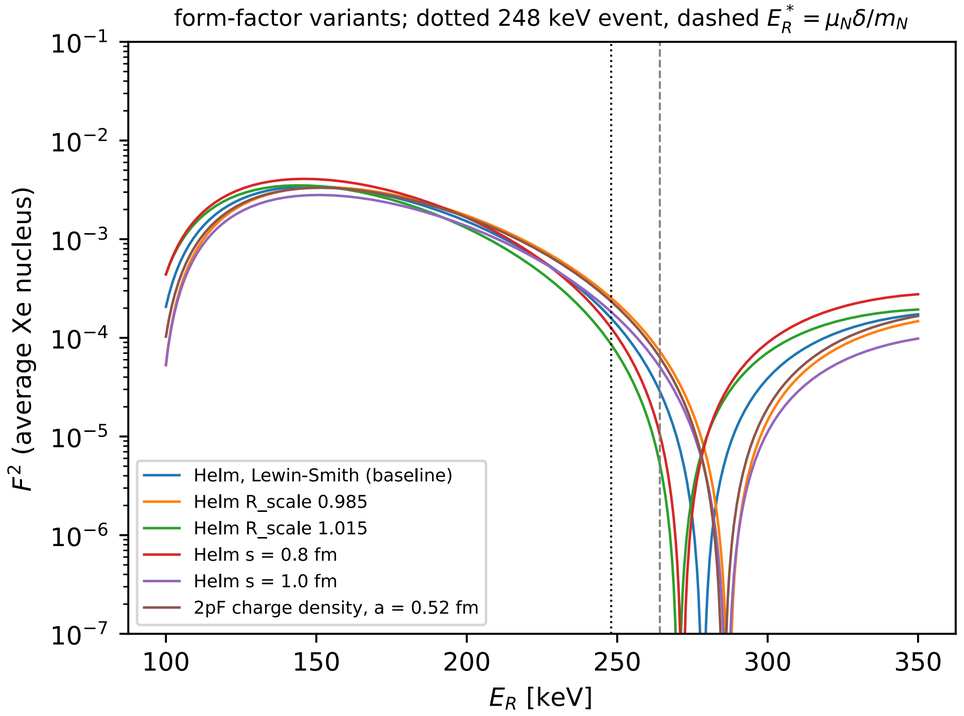
Backup: ϵ dependence

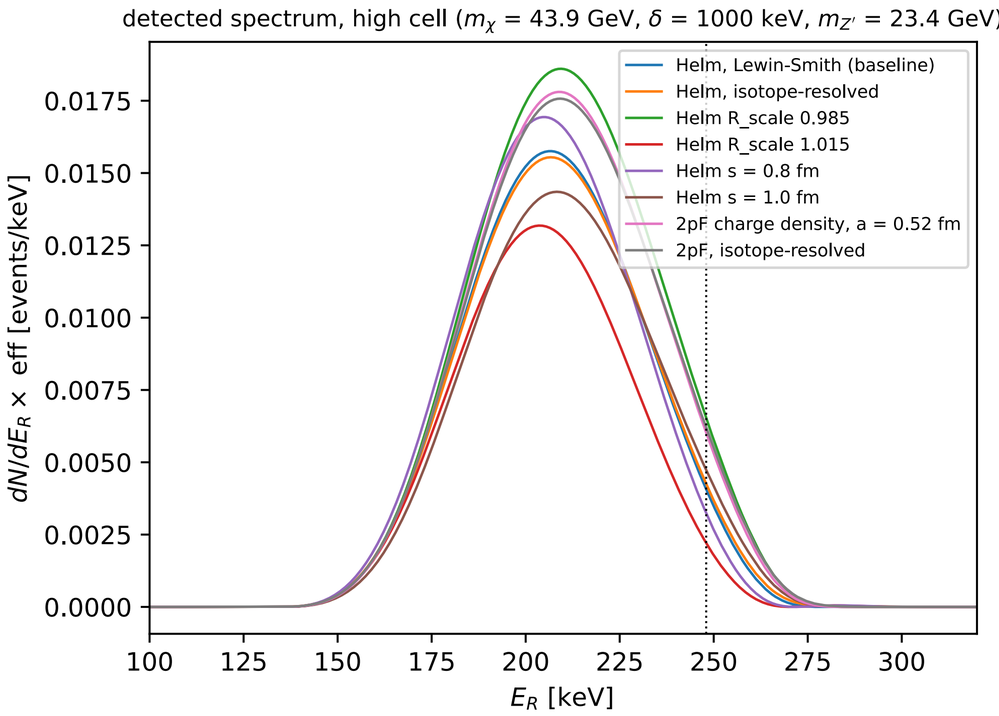
LZ minima in the cell (43.9 GeV, 1000 keV), $\rho_\odot$ = 0.4 GeV/cm³

ϵ	branch	$m_{Z'}$ [GeV]	f_2	$-2 \ln \mathcal{L}$
10^{-3}	low	3.12	1.11×10^{-6}	12.339
10^{-3}	high	no minimum in this cell		
10^{-4}	low	1.050	1.54×10^{-6}	12.342
10^{-4}	high	25.08	0.4971	12.339
10^{-5}	low	0.37	4.23×10^{-6}	12.371
10^{-5}	high	7.6	0.381	12.339

Both $\sigma_{\chi p}$ and Γ_{χ_2} scale as $\epsilon^2 g_X^2 / m_{Z'}^4$, while g_X and the conversion do not depend on ϵ, so that $m_{Z'} \propto \epsilon^{1/2}$ at nearly the same –2 ln $\mathcal{L}$.

Backup: nuclear form factor





The event sits just below the second zero of the xenon form factor. Variants of the Helm form, a two-parameter Fermi density, and the isotope sum change the expected count near the event, but leave the likelihood almost unchanged at the tested LZ-only best-fit point of the $\rho_\odot = 0.3$ scan (held fixed, no refit).

Backup: χ_2 decays below 2m_e

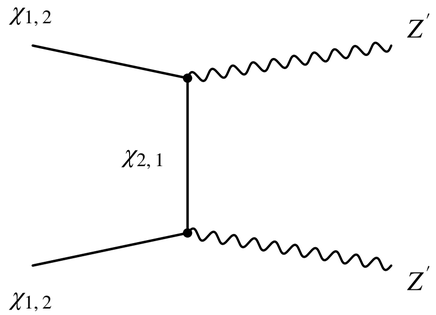
$$\Gamma(\chi_2 \to \chi_1 \nu\bar{\nu}) \simeq \frac{\alpha_{\rm EM}\, g_X^2\, \epsilon^2}{315\pi^2 c_W^2}\, \frac{\delta^9}{m_{Z'}^4\, m_Z^4}$$

$$\Gamma^{\rm EH}(\chi_2 \to \chi_1 + 3\gamma) \simeq \frac{17\, \alpha_{\rm EM}^4\, g_X^2\, c_W^2\, \epsilon^2}{1368241875\, \pi^5}\, \frac{\delta^{13}}{m_e^8\, m_{Z'}^4}$$

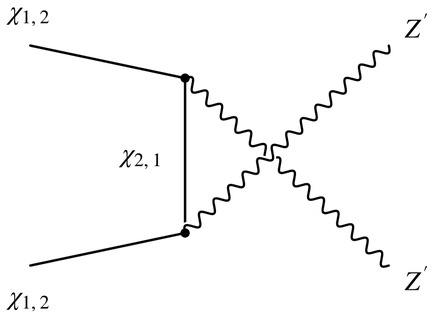
The νν̄ width goes through the Z admixture of the Z' and holds for $\delta \ll m_{Z'}, m_\chi$; the 3γ width comes from the electron loop (Euler–Heisenberg) with the Z'^* propagator and holds for $\delta \ll m_e$. They match Batell et al. (δ^9) and Krnjaic et al. ($g' = g_X$, mixing ϵc_W), and near $2m_e$ we rescale by the full one-loop $Z'^* \to 3\gamma$ width. Both scale as $\epsilon^2 g_X^2 / m_{Z'}^4$, like $\sigma_{\chi p}$, which is the INTEGRAL link.

Batell, Pospelov & Ritz 2009; Pospelov, Ritz & Voloshin 2008; Krnjaic et al. 2025; one loop: McDermott, Patel & Ramani 2018.

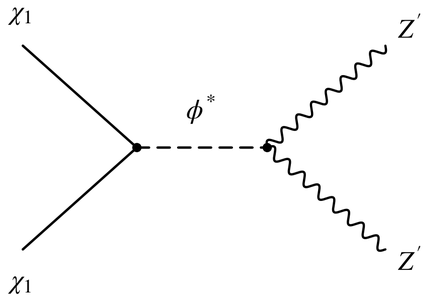
Backup: energy growth and the ϕ exchange



t-channel χ exchange



u-channel χ exchange

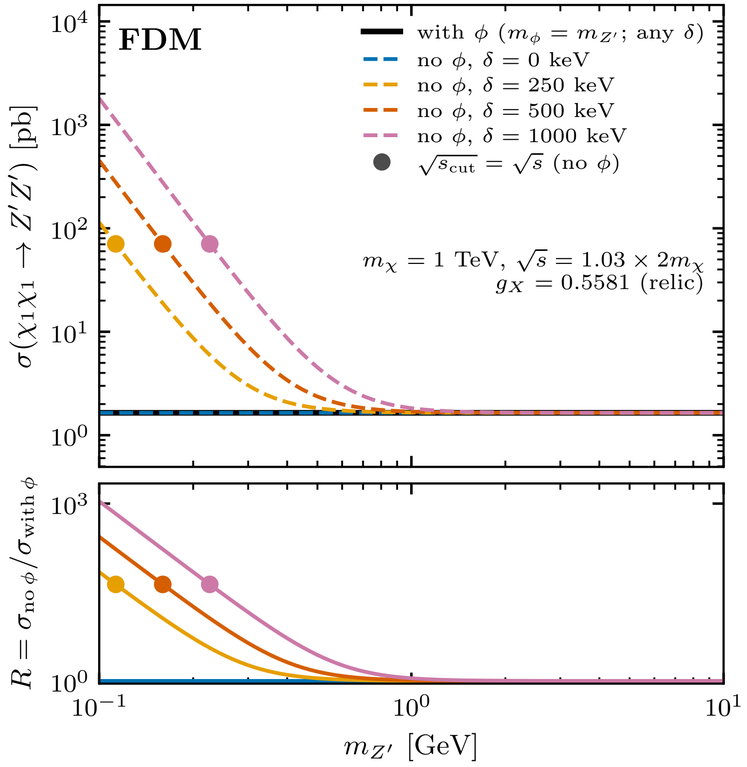


s-channel ϕ exchange

For longitudinal Z' , the t- and u-channel χ exchanges grow with energy, and their sum leaves a growth proportional to δ, because the splitting is a mass term that breaks the gauge symmetry. In the gauge theory, $\mathscr{L} \supset -(g_X\delta/2m_{Z'})[\bar{\chi}_2\chi_2 - \bar{\chi}_1\chi_1] + (m_{Z'}^2/v_\Phi)\phi Z'_\mu Z'^\mu$, and the s- channel ϕ exchange cancels this remainder. This is the Higgs mechanism at work, as for $f\bar{f} \to Z_L Z_L$ in the SM, where Higgs exchange cancels a growth $\propto m_f\sqrt{s}$.

Backup: freeze-out cross section without ϕ

For $\delta \neq 0$, without ϕ the $\chi_1\chi_1 \to Z'Z'$ cross section at a representative freeze-out energy is larger and grows as the Z' gets lighter, even below $\sqrt{s_{\rm cut}}$ (circles); for $\delta = 0$ the two agree. The illustration uses $m_\chi = 1$ TeV and $g_X = 0.56$; at our LZ benchmarks, the energy growth is small, and the two models differ mainly through $Z'\phi$ and the resulting g_X .



$\chi_1\chi_1 \to Z'Z'$ at $\sqrt{s}/2m_\chi = 1.03$; circles: $\sqrt{s} = \sqrt{s_{\rm cut}}$

Figure: Fig. S1 (right) of our paper.

Backup: h → Z′Z′

$$\Gamma(h \to Z' Z') = \frac{\lambda_{Z'H}^2 v_H^2 m_h^3}{32\pi\, m_{Z'}^4} \left(1 - \frac{4m_{Z'}^2}{m_h^2} + \frac{12 m_{Z'}^4}{m_h^4}\right) \left(1 - \frac{4m_{Z'}^2}{m_h^2}\right)^{1/2}$$

Without the gauge symmetry the coupling $\lambda_{Z'H} Z'_\mu Z'^\mu H^\dagger H$ is allowed, and at fixed $\lambda_{Z'H}$ the width diverges as $m_{Z'} \to 0$ through the longitudinal Z'_L : the simplified model is an effective theory whose cut-off vanishes as $m_{Z'} \to 0$. In our model $|\lambda_{Z'H}| = |s_\alpha| m_{Z'}^2/(v_H v_\Phi)$ follows from the $h - \phi_0$ mixing, so $\Gamma \simeq s_\alpha^2 m_h^3/(32\pi v_\Phi^2)$ stays finite as $m_{Z'} \to 0$, both for $g_X \to 0$ at fixed v_Φ and for $v_\Phi \to 0$ (then $s_\alpha \propto v_\Phi$), and is negligible for s_α = 10^{-6}.

Baek, Ko & Park 2022; Baek, Ko, Park & Senaha 2013.

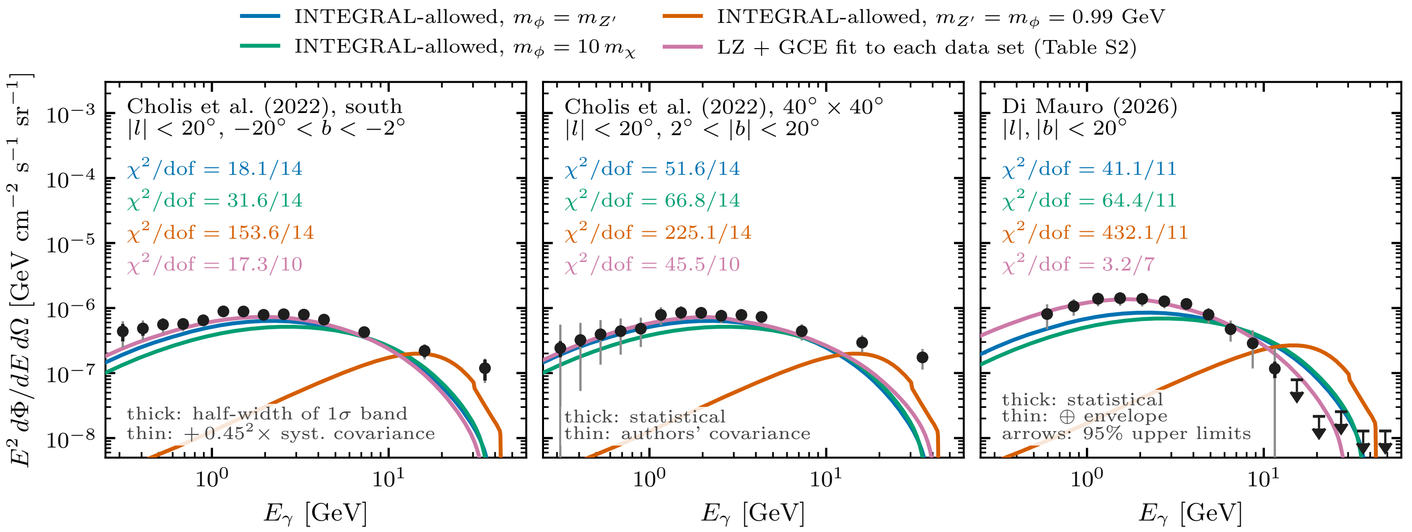
Backup: joint fits per data set

Q = –2 ln $\mathcal{L}$_LZ + χ²_GCE minimized over $(m_\chi, \delta, m_{Z'}, m_\phi)$, A = 1 unless stated, no INTEGRAL limit

	χ^2/bins, nothing fitted		joint fit					
data set	benchmark	no ϕ ($m_\phi = 10\, m_\chi$)	m_χ [GeV]	δ [keV]	$m_{Z'}$ [GeV]	m_ϕ [GeV]	$\chi^2_{\rm GCE}$	$\Delta(-2\ln\mathcal{L}_{\rm LZ})$
South	18.1/14	31.6/14	39.5	1000	27.6	19.5	17.3	0.23
South, free $A = 1.12$	—	—	43.9	1000	27.6	39.0	16.8	0.08
Full window	51.6/14	66.8/14	43.9	800	53.2	13.3	45.5	4.05
Di Mauro 2026	41.1/11	64.4/11	32.0	1000	29.3	14.7	3.2	1.24

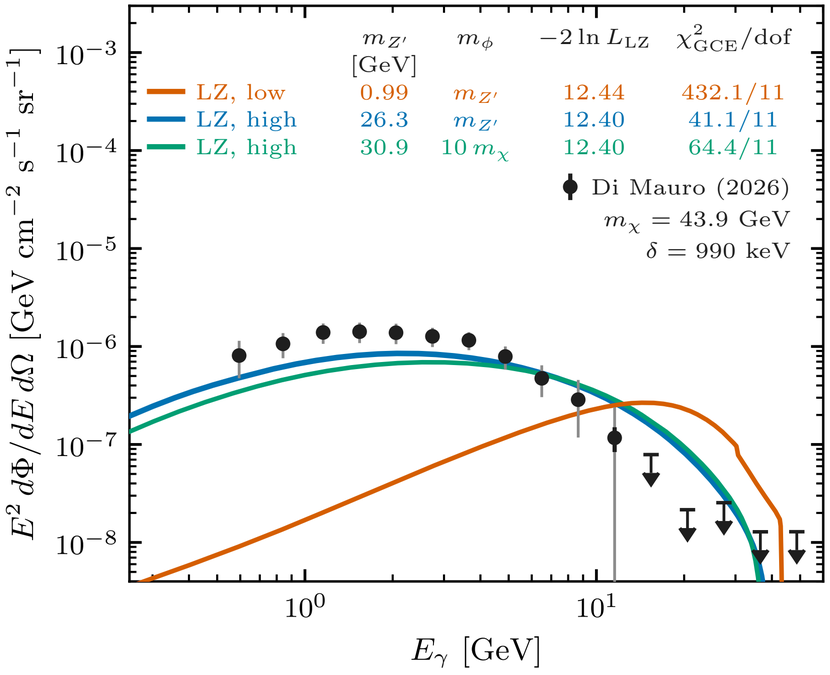
The benchmark is the INTEGRAL-allowed high branch, and the no-ϕ column is the same (m_χ, δ) with $m_\phi = 10 m_\chi$. The joint-fit values are descriptive, not goodness-of-fit measures. LZ and the GCE are jointly compatible in the south and, with independent envelope errors, for Di Mauro, at different m_χ ; not in the full window.

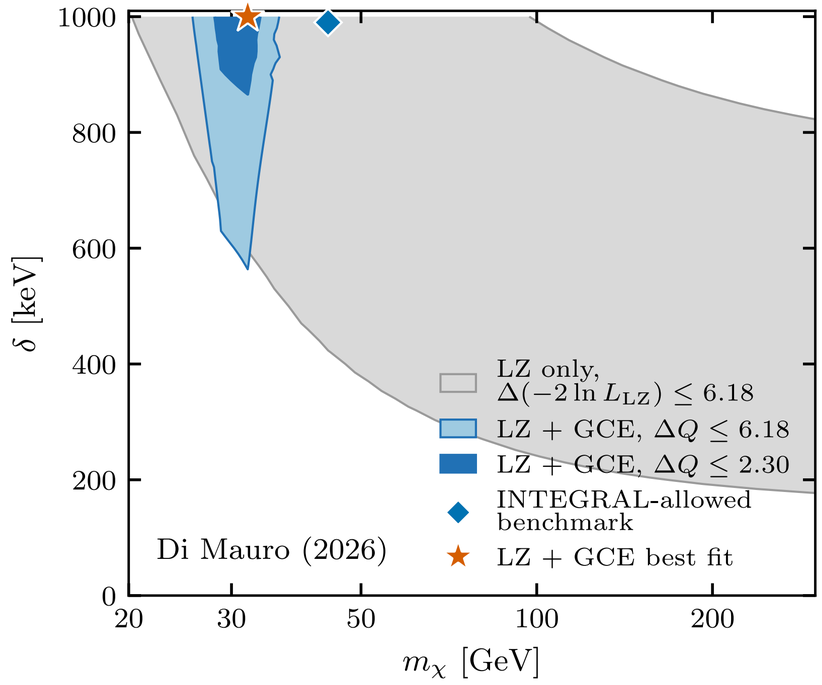
Backup: other GCE data sets



In the full window, which includes the gas-bright north, the benchmark gives 51.6/14 and the generic $b\bar{b}$ fit 50.5/12. On the spectrum of Di Mauro 2026, the benchmark gives 41.1/11 with nothing fitted, and the joint fit (purple) reaches $\chi^2 = 3.2$ at Δ(–2 ln $\mathscr{L}$_LZ) = 1.24, given independent envelope errors. In the full window, the joint fit gives χ^2 = 45.5 at Δ(–2 ln $\mathscr{L}$_LZ) = 4.05.

Backup: Di Mauro 2026 spectrum





Left: the INTEGRAL-allowed benchmarks on the Di Mauro spectrum; nothing fitted. Right: the joint LZ + GCE region, which moves to a lighter m_χ ; it needs independent envelope errors.

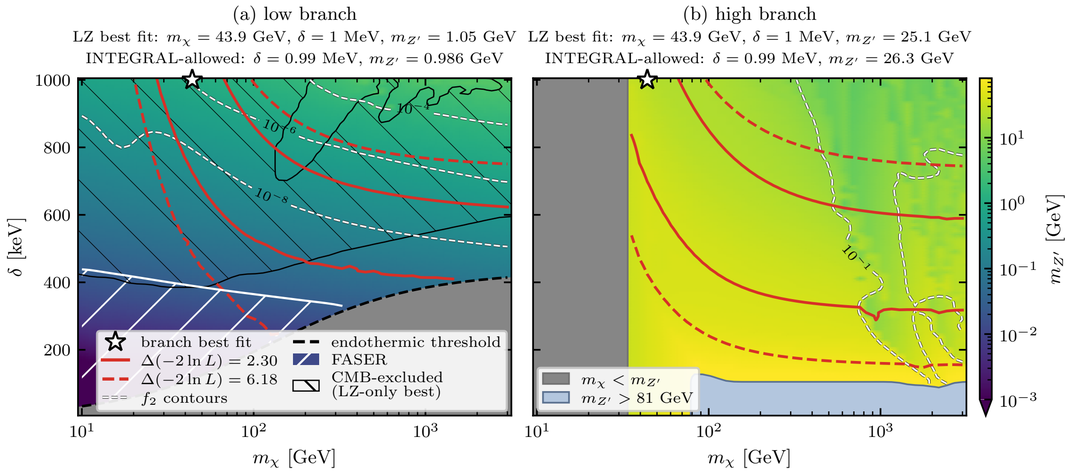
Di Mauro 2026.

Backup: GCE caveats (beyond the manuscript)

Our χ^2 uses the statistical errors plus the authors' systematic principal components, with the systematic part scaled by $(0.45)^2$ in the south, following Cholis et al. The ΔQ regions localize the fit; they are not goodness-of-fit tests. At the benchmark, σv sits at 1.23× the dwarf-spheroidal limit, within the extension uncertainty, and a rescaling of published AMS-02 antiproton limits to our cascade spectrum, done for earlier benchmark points, suggests a possible tension; there is no dedicated AMS-02 analysis.

GCE covariance: Cholis et al. 2022. Dwarf limits: McDaniel et al. 2024 (Fermi-LAT).

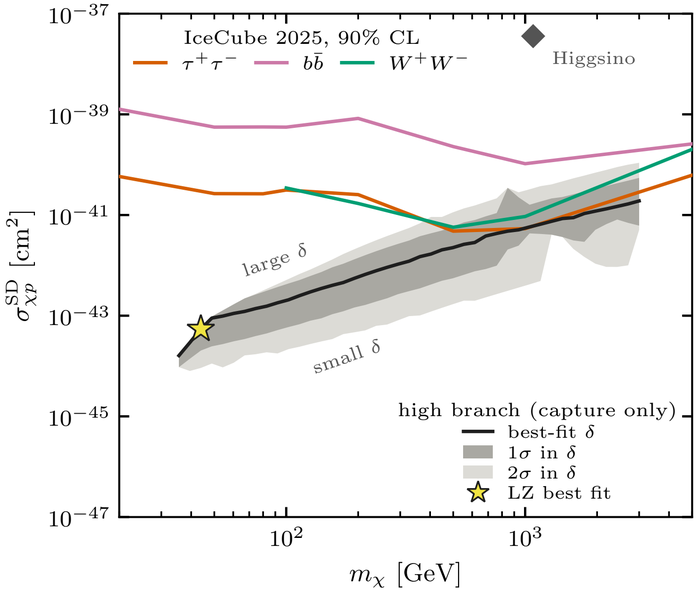
Backup: visible dark-photon limits

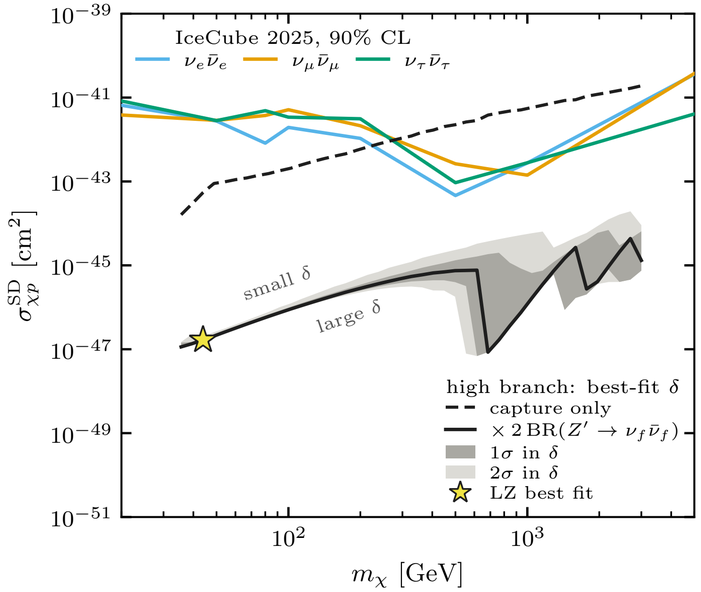


Since $Z' \to \chi_1\chi_2$ is closed, the Z' decays visibly, with coupling $\epsilon c_W e$. The preliminary FASER search (white hatching) reaches only the small-δ corner of the low branch, and near the benchmarks, the coupling lies below the BaBar and KLOE limits (low) and the LHCb and CMS limits (high). At the benchmarks the dark Higgs decays before BBN for $\sin\alpha = 10^{-6}$.

FASER Collaboration 2026 (preliminary); BaBar 2014; KLOE-2 2018; LHCb 2020; CMS 2020; ϕ decays: Winkler 2019.

Backup: solar neutrinos





Left: capture-equivalent spin-dependent cross section along the high branch against the IceCube limits for single annihilation channels. Right: the direct neutrino channel from $Z' \to \nu\bar{\nu}$. Capture only (annihilation and equilibrium not modelled), $\rho_\odot = 0.3$ scan; the right panel compares our softer cascade neutrinos with line-channel limits. The LZ best fit lies far below; at TeV masses, the band reaches the $\tau^+\tau^-$ and W^+W^- limits.

IceCube 2025; Higgsino capture: Di Mauro & Shaikh.

Backup: scalar inelastic DM

Inelastic scalar dark matter, a complex scalar in a similar dark $U(1)_X$ model, could explain the event too, because the exothermic kinematics depends only on (m_X, δ) . But it has a different excited-state fraction f_2 , a different relic density and several additional quartic couplings in the scalar potential. We leave this case for future work.

Related scalar models: Baek, Ko & Park 2015 (GCE); Baek, Kim & Ko 2025 (U(1)_(L_μ−L_τ)).